ON THE CONSTRUCTION OF NON-ORTHOGONAL LINEAR SPACE-TIME BLOCK CODES

by

Shant Sethian

A thesis submitted to the

Department of Mathematics and Statistics

in conformity with the requirements

for the degree of Master of Science (Engineering)

Queen's University

Kingston, Ontario, Canada

October 2005

Abstract

Space-time block codes (STBCs) with orthogonal designs, called orthogonal space-time block codes (OSTBCs), provide an elegant encoding and linear decoding technique while offering full diversity benefits in multiple-input multiple-output (MIMO) environments. Unfortunately, OSTBCs are difficult to design as the number of transmit antennas increases and, other than Alamouti's two-branch diversity scheme, do not achieve full rate. Non-orthogonal STBCs (NOSTBCs) relax orthogonality conditions in code design, leading to exponential decoding complexity in exchange for higher rates.

In this work, we propose a NOSTBC design based on the linear dispersion code (LDC) framework, providing high rates for any number of antennas. Our design aims to improve frame error rate (FER) performance, compared to well-known STBCs, by iteratively choosing code design parameters that minimize the union upper bound on the FER. This design technique is implemented with three different initialization codes: Alamouti's code, the V-BLAST code and an LDC code.

For the initialization with Alamouti's code, new codes with tighter FER upper bounds were found for the cases of 2 and 4 receive antennas. For the V-BLAST and LDC initializations, an improved FER upper bound was found for the cases of 1, 2 and 4 receive antennas.

Simulations show that the new Alamouti-initialized codes outperform Alamouti's code in terms of FER and BER at an increasing rate as the number of receive antennas is increased. The new V-BLAST-initialized codes outperformed V-BLAST in FER and BER at a diminishing rate as the number of receive antennas increases. Finally, the new LDC-initialized codes outperformed the LDC code in FER and BER for the case of 1 receive antenna but no conclusive frontrunner was seen for the cases of 2 and 4 receive antennas, since the error rate computations were too small to be reliable for higher CSNRs.

The results show that our non-orthogonal codes, designed by minimizing the FER union upper bound, produce strong FER and BER performances over a range of receive antennas and CSNRs when compared with the selected STBCs. This error rate improvement comes at the cost of exponential decoding complexity, compared to linear decoding complexity for orthogonal codes.

Acknowledgements

This thesis is a culmination of the contributions of many individuals who supported me, directly or indirectly, in the past few years.

Firstly, I would like to thank my supervisors, Dr. Fady Alajaji and Dr. Tamas Linder, for their ongoing support and encouragement: particularly in times when I took an unexpected detour from my research. Without their commitment this thesis would not have been written. I also thank my wonderful family for their unwavering faith in me during times when the finish-line was not in sight. *Verchabes eree!* To my friends - thank you for the laughs, distractions, motivation and memories. You made the journey a much easier one.

Finally, a very special thank you to Dr. Firouz Behnamfar. Without his selflessness, insight, teaching abilities and contagious enthusiasm for the subject, this Master's thesis simply would not have materialized.

Thank you all. *Shnorhagal-em.*

Contents

List of Tables

List of Figures

Chapter 1

Introduction

1.1 Motivation

With an increasing demand for reliable cellular and wireless data applications, such as wireless Internet, email and multimedia applications, there is a rising need for high data rate wireless communication. As users' demands exceed the capacity of wireless networks, operators are forced to find ways to improve the network capacity and throughput in order to provide an acceptable level of service.

Unlike wired channels, which are static and predictable, wireless channels can be unreliable since they are subjected to time-varying impairments such as noise, interference and *multipath propagation*. Multipath causes a transmitted signal to reach the receiver from two or more paths due to

refraction and reflection off of terrestrial objects, such as mountains and buildings. As these scattered waves make their way to the receiver, they cause constructive and destructive interference and phase shifting in the signal, which ultimately lead to increased receiver errors [16][20].

A proven way to mitigate these effects is by employing *diversity* techniques. In essence, diversity amounts to creating redundancy in the transmitted signal with the expectation that the different transmissions will undergo different fading. This provides the receiver with multiple versions of the same information. Current diversity techniques include *space* (or *antenna*) diversity, *frequency* diversity and *time* diversity. Space diversity uses two or more physically separated antennas to create multiple independent fading channels. Frequency diversity takes advantage of the fact that different carrier frequencies, sufficiently spaced out, will undergo different fading and multipath characteristics over a channel. In time diversity, signals representing the same information are sent over the channel at different times, under different channel fading conditions [24][20].

Recent breakthroughs in digital signal processing have allowed wireless communication systems to utilize both space and time diversity to address system performance needs by employing multiple-antennas at the transmitter and/or receiver to create a system with independently fading channels. A system employing more than one transmitting and more than one receiving antenna is called a *multiple-input*, *multiple-output* (MIMO)

system. MIMO systems have been shown to increase the system capacity as the number of transmit and receive antennas increases, when compared with *single-input, single-output* (SISO) systems [26][8].

Space-time coding is a technique used in MIMO communications as a means to exploit the full diversity benefits of a multi-antenna system by utilizing both space and time diversity to transmit information. The design of these codes takes into account a trade-off between decoding complexity at the receiver, maximizing the information rate and minimizing decoding errors [16].

A popular family of *space-time codes* (STCs) is the class of *space-time block codes* (STBCs). STBCs operate on a block of input symbols, producing a matrix whose columns represent antennas and rows represent time. These codes generally do not offer *coding gain* but their main advantage comes from the fact that they can provide full *diversity gain* with relatively simple encoding and decoding schemes, compared with trellis-based codes. One category of STBCs, called *orthogonal space-time block codes* (OSTBCs), follow orthogonal designs in code construction, providing linear-time decoding. Unfortunately, the design of these codes for an arbitrary number of transmit antennas with rates greater than 1/2 is quite difficult.

There is also a class of *non-orthogonal space-time block codes* (NOSTBCs) which relax the orthogonality conditions in exchange for higher information

rates. One such family of NOSTBCs are *linear dispersion codes* (LDCs) (or linear-STBCs) which break the input data into substreams which are then dispersed in linear combinations over space and time [11]. LDCs offer many of the advantages of OSTBCs but remain relatively easy to design for any number of transmit and receive antennas.

1.2 Literature Review

One of the pioneering papers on STBC design was Alamouti's 1998 description of a two-branch transmit diversity scheme, which he generalized for any number of receive antennas [1]. The code design followed an orthogonal block structure, providing a diversity advantage of $2n_R$, where n_R is the number of receive antennas. Recognizing the potential of this technique, Tarokh *et al.* extended Alamouti's work in [25] by creating generalized STCs with orthogonal block coding structure, called orthogonal space-time block codes. In their work, Alamouti's scheme was generalized for any number of transmit antennas for real and complex constellations. A major result of their work was the recognition, via the *Hurwitz-Radon theorem*, that full-rate OSTBCs do not exist for $n_T > 2$, where n_T is the number of transmit antennas, making Alamouti's code a unique OSTBC. Generalized complex OSTBC design guidelines were proposed which achieved a rate 1/2 while a few sporadic codes that achieved rate 3/4 with three and four transmit antennas were presented. More recently, Su *et al.*

[22] found generalized complex OSTBCs with rate 7/11 and 3/5 for the case of five and six transmit antennas and Kan *et al.* [15] presented a rate 5/8 code employing eight transmit antennas.

Alternatively, non-orthogonal STBCs emerged as a way to overcome the shortcoming of orthogonal designs in the sense of full rate attainability for a higher number of transmit antennas. The *Bell Labs Layered Space-Time* (BLAST) codes, first introduced by Foschini [7] (diagonal-BLAST) and later modified by Wolniansky *et al.* in [27] (vertical-BLAST), utilize a non-orthogonal coding technique which divides the input bit stream into substreams that are layered diagonally or vertically over space and time. In 2002, Hassibi *et al.* presented in [11] a new type of NOSTBC design which is linear over space and time. These so-called linear dispersion codes offer high performance gains using any number of transmit and receive antennas via a design technique which aims to maximize the mutual information between the transmitted symbols and received symbols. More recently, Heath *et al.* [12] proposed an LDC which jointly considers the ergodic capacity (via mutual information) and diversity advantage (via the *rank* and *determinant criterion* in [24]) in code design. The LDC framework forms the basis for the new NOSTBCs designed in this work.

Naturally, it is desirable to quantify the "goodness" of our STCs. Two such measurements are the *frame error rate* (FER) (also called the *codeword error rate* (CWER)) and the *bit error rate* (BER). Both FER and BER can be

expressed in terms of the probability of a union of N (finitely-many) events, $P(A_1 \cup \ldots \cup A_N)$. Due to the infeasibility of finding this probability outright, an upper bound for the probability of a union, known as the *union bound* [26, 4.2.4] is commonly used in its place. The union bound bounds the probability of a union from above by summing the individual terms $P(A_i)$ for $i = 1,\ldots,N$. In the context of error probabilities, we define each event as the receiver decoding erroneously in favor of a codeword $\hat{\mathbf{S}}$ when $\mathbf{S}$ was transmitted in a system with only two codewords. The probability of this event is known as the *pairwise error probability* (PEP) and is denoted by $P(\mathbf{S} \to \hat{\mathbf{S}})$. Many authors have found upper and lower bounds to the PEP in lieu of a direct computation, such as Lu *et al.* in [17] and Tarokh *et al.* in [24]. However, this work will use an exact expression for the PEP as given by Behnamfar *et al.* in [2][3], which relies on the residues of the moment generating function (MGF) of the squared-distance between a pair of codewords. This PEP expression is used in the union bound to form an upper bound on the FER for newly designed non-orthogonal linear-STBCs.

1.3 Contributions

The contribution of this thesis is a design technique for linear-STBCs based on iteratively improving the frame error rate performance by optimizing the codeword design parameters to minimize the FER union upper bound. The new codes are formed via an initialization with three well-known STBCs:

Alamouti's OSTBC from [1], the V-BLAST code from [27] and an LDC presented in [11]. These new codes are then tested in a computer simulation where the FER and BER are computed, plotted and compared with the codes used to form them for a range of CSNRs and a varying number of receive antennas.

1.4 Thesis Outline

The remainder of this thesis is organized as follows. In Chapter 2, background on communication channel models and fundamental results of information theory are provided followed by a multi-antenna communication system model. The chapter introduces the fundamental concepts and results of space-time block coding with a particular focus on OSTBCs and linear-STBCs. The design tradeoff between orthogonal and non-orthgonal codes is also discussed. An exact PEP expression is introduced which forms the foundation for the error rate calculations in the new code design. Chapter 3 begins with a derivation of the error probability expression that is used in our code design. The new code design technique is described and the formation of new NOSTBCs via initialization with three well-known codes is presented at the end of the chapter along with the FER union upper bound results. These newly designed codes are then compared via simulation with the codes used to form them and the results are presented

and discussed in Chapter 4. Finally, in Chapter 5, the findings are summarized and future research opportunities are proposed.

Chapter 2

Space-Time Block Codes

2.1 Channel Models and Information Theory Results

2.1.1 Channel Models

When working with communication systems, one needs to define a channel model to emulate the environmental conditions that will govern the communication process. Two such channel models are the *AWGN* channel and the *Rayleigh fading* channel.

AWGN Channel

The *additive white Gaussian noise* (AWGN) channel provides a simplistic view of a communication channel by modeling the presence of noise without accounting for distortion due to signal fading.

The AWGN channel is a discrete-time channel with continuous input and output alphabets. At time t, the channel output Y_t is defined as [4]

$$Y_t = X_t + V_t \ , \tag{2.1}$$

where X_t is the transmitted signal and is independent of V_t, which is the i.i.d. additive noise term with Gaussian distribution and covariance matrix $\mathbf{\Phi}_V = \mathrm{E}[\mathbf{V}\mathbf{V}^*] = \sigma^2 I_{n_R}$, where $(\cdot)^*$ represents complex conjugation.

Rayleigh Fading Channel

A more realistic representation of a communication channel, particularly in a wireless environment, is the Rayleigh fading channel. This channel model takes into account signal fading incurred during transmission due to multipath propagation. At time t, the channel output Y_t is defined as [21]

$$Y_t = H_t X_t + V_t \ , \tag{2.2}$$

where X_t, V_t and H_t are independent, with the former two defined as in the AWGN case. H_t denotes the signal attenuation factor due to the communication environment with its coefficients having Rayleigh distribution with a *probability density function* (pdf) given by

$$f_H(a) = \begin{cases} 2ae^{-a^2} & \text{, if } a > 0 \\ 0 & \text{, otherwise.} \end{cases} \tag{2.3}$$

2.1.2 Some Results from Information Theory

Mutual Information

We first define the mutual information $I(\mathbf{X};\mathbf{Y})$ between two continuous random variables $\mathbf{X}$ and $\mathbf{Y}$ as [4]

$$I(\mathbf{X};\mathbf{Y}) = \int_{\mathbf{R}^N} \int_{\mathbf{R}^M} p(\mathbf{x},\mathbf{y}) \cdot \log\left(\frac{p(\mathbf{x},\mathbf{y})}{p(\mathbf{x})p(\mathbf{y})} \right) dydx\,, \tag{2.4}$$

where N and M are the dimensions of $\mathbf{X}$ and $\mathbf{Y}$, respectively, $p(\mathbf{x},\mathbf{y})$ is the joint pdf and $p(\mathbf{x})$ and $p(\mathbf{y})$ are the pdfs of $\mathbf{X}$ and $\mathbf{Y}$, respectively. In words, the mutual information measures the amount of information in $\mathbf{X}$ that is shared with $\mathbf{Y}$. It can be shown that if $\mathbf{X}$ and $\mathbf{Y}$ are independent, there will be no mutual information between them, that is $I(\mathbf{X};\mathbf{Y}) = 0$. Examining (2.4) one can verify that $I(\mathbf{X};\mathbf{Y}) \geq 0$ for any $\mathbf{X}$ and $\mathbf{Y}$.

Capacity

The *information capacity* of a communication channel with transmit signal covariance matrix $\mathbf{\Phi}_X = \mathrm{E}[\mathbf{X}\mathbf{X}^*] = {P}/{n_T}\, I_{n_T}$ under a power constraint P is defined as

$$C = \sup_{p(\mathbf{x}):\, \mathrm{tr}(\mathbf{\Phi}) \leq P} I(\mathbf{X};\mathbf{Y}) \quad \text{bits/channel use,} \tag{2.5}$$

where $\mathbf{Y}$ is the received signal. The supremum is taken over all input pdfs that satisfy the given power constraint.

The *channel rate* R_c represents the number of bits per transmission and is said to be "achievable" if information can be transmitted at rate R_c with an arbitrarily low probability of error [4]. The *operational capacity* of a channel is defined as the supremum of all achievable rates. Shannon proved that the information capacity in (2.5) and the operational capacity are equal [4] and will herein be referred to simply as *capacity*.

It was shown in [26][16] that the capacity of an AWGN channel with SISO is given by

$$C = \mathrm{E}_h\left[\log_2\left(1+\frac{P}{\sigma^2}\left|h_{1,1}\right|^2\right)\right] \quad \text{bits/channel use,} \tag{2.6}$$

where $\mathrm{E}_h[\cdot]$ represents the expected value averaged over h, P/σ^2 is called the *channel signal-to-noise ratio* (CSNR) and denoted by γ_s and $h_{1,1}$ is the channel gain between the transmitter and receiver. The input distribution that maximizes the capacity (mutual information) is a circularly symmetric complex Gaussian random variable [26].

For a Rayleigh fading channel, beginning with expression (2.5) under a power constraint, the authors in [21] show the capacity of a MIMO channel with n_T transmit antennas and n_R receive antennas is given by

$$C = \mathrm{E}_{\mathbf{H}}\left[\log_2[\det(\mathbf{I}_{n_R} + \frac{\gamma_s}{n_T}\mathbf{H}\mathbf{H}^{\mathrm{t}}] \right] \quad \text{bits/channel use,} \tag{2.7}$$

where $\mathrm{E}_{\mathbf{H}}[\cdot]$ represents the expected value averaged over the channel matrix $\mathbf{H} = [h_{j,i}]$, $\mathbf{I}_{n_R}$ is the $n_R \times n_R$ identity matrix and $(\cdot)^{\mathrm{t}}$ is the Hermitian transpose. The path gains $h_{j,i}$ between transmit antenna i and receive antenna j, for $i = 1,...,n_T$ and $j = 1,...,n_R$, are complex Gaussian with Rayleigh fading coefficients with pdf (2.3).

To evaluate the effect on capacity of increasing the number of transmit and receive antennas, Grant [9] produced an upper bound on (2.7), which is tight for high CSNRs, and found

(a) For a fixed n_T, as n_R is increased there is an asymptotically logarithmic increase in capacity with n_R.

(b) For a fixed n_R, as n_T is increased there is no capacity improvement, though this does help to eliminate fading effects.

(c) For a ratio $n_T / n_R = \beta \leq 1$, as n_T and n_R grow a linear capacity increase occurs.

(d) For a $\beta > 1$, there is no asymptotic increase in capacity associated with growing n_T beyond n_R.

Diversity and Coding Gain

Increased channel capacity of MIMO systems with respect to SISO systems can be partly realized through space-time coding, which can provide

diversity and *coding* gains. Diversity gain is a measure of the advantage gained by using diversity techniques – such as space, time or frequency diversity – versus a traditional SISO system where no diversity is employed. Coding gain is a measure of the advantage of a given code when compared with an uncoded system under identical system conditions.

In [24], the authors quantify the diversity and coding gain by first forming a Chernoff upper bound on the PEP in terms of the matrix $\mathbf{U}$ defined by

$$\begin{aligned} d_{i,t} &= s_t^i - \hat{s}_t^i \\ u_{k,i} &= \sum\nolimits_t d_{i,t} d_{k,t}^* \\ \mathbf{U} &= \left[u_{k,i} \right] \end{aligned}$$

for $1 \le i,k \le n_T$, where s_t^i and $\hat{s}_t^i$ are the symbols of the codewords $\mathbf{S}$ and $\hat{\mathbf{S}}$ at time t from antenna i, respectively. Letting $r \le n_T$ be the rank of $\mathbf{U}$, then the kernel of $\mathbf{U}$ has dimension $n_T - r$ with $n_T - r$ eigenvalues. Taking only its r positive eigenvalues $\lambda_1, \ldots, \lambda_r$, the worst-case PEP upper bound is written as

$$P\left(\mathbf{S} \to \hat{\mathbf{S}}\right) \le \left(\prod_{i=1}^{r} \lambda_i \right)^{-n_R} \left(\frac{\gamma_s}{4} \right)^{-r \cdot n_R} , \tag{2.9}$$

which provides a diversity gain of $r \cdot n_R$ and a coding gain of $\left(\lambda_1 \lambda_2 \cdots \lambda_r\right)^{1/r}$ [24]. In order to achieve maximal (or full) diversity gain, the matrix $\mathbf{U}$ should be full-rank, that is $r = n_T$, to produce a diversity advantage of $n_T \cdot n_R$.

2.2 System Model

We begin our discussion of space-time codes by formally establishing a multiple-antenna communication model to be used throughout this work (Fig. 2.1). Consider a system with n_T transmit and n_R receive antennas where an i.i.d. uniform input bit stream $\mathbf{b} = [b_1,...,b_m]$ is mapped to a constellation of size $M = 2^m$ (with unit energy) which is used to form the baseband signals s to encode into blocks $\mathbf{S}$. To ensure a CSNR of γ_s at each receive antenna, the symbols are weighted by $\sqrt{\frac{\gamma_s}{n_T}}$ so that transmit antenna i sends $\sqrt{\frac{\gamma_s}{n_T}} s_t^i$ at time t. The channel induces Rayleigh flat fading with the complex path gain from transmit antenna i to receive antenna j denoted $h_{j,i}$, which are zero-mean, unit-variance complex Gaussian random variables, denoted by $\mathcal{CN}(0,1)$, with i.i.d. real and imaginary parts.

Figure 2.1 – Space-time communication model

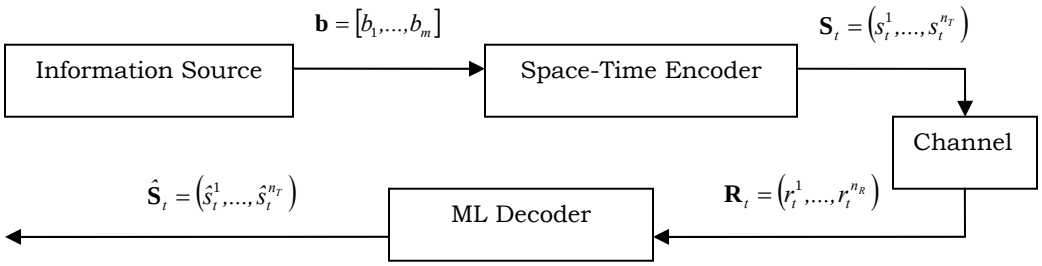

The path gains $h_{j,i}$ are known to the receiver but not the transmitter and the channel is *quasi-static*, meaning the path gains are constant within a symbol period T but vary from one symbol period to the next. The received signal at antenna j at time t can be written as

$$r_t^j = \sqrt{\frac{\gamma_s}{n_T}} \sum_{i=1}^{n_T} h_{j,i} s_t^i + v_t^j \ , \tag{2.10}$$

for $j = 1,...,n_R$, $t = 1,...,l$ where l is the frame length, and where v_t^j is the additive noise term seen at antenna j at time t with $\mathcal{CN}(0,1)$ distribution and i.i.d. real and imaginary parts. Defining $\mathbf{R}_t = \left(r_t^1,...,r_t^{n_R}\right)^{\mathrm{T}}$, $\mathbf{S} = \left(s_t^1,...,s_t^{n_T}\right)^{\mathrm{T}}$, $\mathbf{V}_t = \left(v_t^1,...,v_t^{n_R}\right)^{\mathrm{T}}$, where $(\cdot)^{\mathrm{T}}$ denotes transposition, and $\mathbf{H}_{n_R \times n_T} = \lfloor h_{j,i} \rfloor$, (2.10) can be expressed in matrix form as

$$\mathbf{R}_t = \sqrt{\frac{\gamma_s}{n_T}} \mathbf{H}\mathbf{S} + \mathbf{V}_t \ . \tag{2.11}$$

With all codewords being equally likely, the *maximum likelihood* (ML) decoder at the receiver computes

$$\hat{\mathbf{S}} = \underset{\mathbf{S}}{\operatorname{argmin}} \left\| \mathbf{R} - \sqrt{\tfrac{\gamma_s}{n_T}} \mathbf{H}\mathbf{S} \right\|^2 , \tag{2.12}$$

where $\hat{\mathbf{S}}$ represents the codeword with the lowest decision metric out of all possible codewords in the codebook.

2.3 Space-Time Diversity

The benefits of space-time coding stem from its utilization of space and time diversity at both the receiver and the transmitter. *Receive diversity* (Fig. 2.2) is well-established in current wireless systems as a way of exploiting space diversity by employing multiple antennas on the receiving-end of the *uplink* (from the mobile to the base station). Based on the well-known *maximal receive ratio combining* (MRRC) method, the received signals are digitally combined and decoded [1][20]. The inherent diversity gain, proportional to the number of receive antennas n_R, results in considerable performance improvements in terms of a better link budget and tolerance for *co-channel interference* [16][19]. Another major advantage to receive diversity is that the improvement in uplink quality comes without incurring additional cost, size or power constraints on the mobile unit.

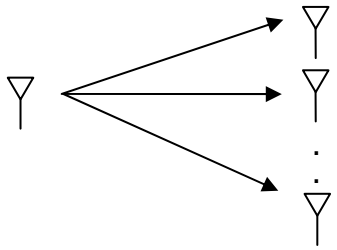

Figure 2.2 – Receive diversity

More recently, *transmit diversity* (Fig. 2.3) has received a lot of attention as a means to achieve the same performance benefits offered through receive diversity. A major obstacle in transmit diversity schemes is to accurately

reflect the current channel conditions, called the *channel state information* (CSI), when transmitting. There are three broad categories according to which CSI updates are carried out: (i) those that use feedback from the receiver to the transmitters, (ii) those that use training information from the transmitters to the receiver and (iii) blind schemes, which use no training or feedback information between the transmitters and receiver [24].

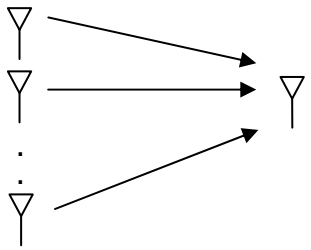

Figure 2.3 – Transmit diversity

MIMO systems (Fig. 2.4) provide a combination of transmit and receive diversity by employing multiple antennas at both sides of the communication system. The remainder of this chapter will look at a category of codes designed to exploit the MIMO diversity environment, called space-time codes (STCs).

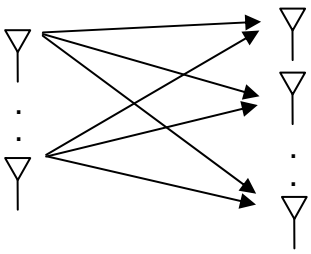

Figure 2.4 – MIMO diversity

2.4 Space-Time Coding

The most prevalent space-time codes can be divided into two main categories: space-time trellis codes (STTCs) and space-time block codes (STBCs). STTCs, discovered by Tarokh *et al.* in 1998 [24], transmit multiple, redundant copies of a trellis (or convolutional) code distributed over time and multiple antennas. STTCs encode a stream of data $s(n)$ via n_T convolution encoders (or one convolution encoder with n_T outputs) and transmit the n_T streams of data $s_1(n),...,s_{n_T}(n)$ via the n_T transmit antennas. These codes provide both coding gain and diversity gain, however, being based on trellis codes they are relatively complex to encode and decode, since they rely on a *Viterbi* decoder at the receiver [10][24].

STBCs, on the other hand, operate on a block of input symbols at a time forming a matrix structure whose rows represent time and columns represent transmit antennas. Unlike STTCs, STBCs generally do not provide any coding gain (unless concatenated with an outer-code) but do provide full diversity benefits [25]. The most attractive feature of STBCs is the relatively simple encoding and decoding scheme.

In the next few sections we will introduce the two classes of STBCs – OSTBCs and NOSTBCs.

2.5 Space-Time Block Codes

A STBC can be viewed as a mapping of n_s complex symbols $\{s_1, \cdots, s_{n_s}\}$ to a matrix $\mathbf{S}$ with dimensions $T \times n_T$, where T is the symbol period and n_T is the number of transmit antennas. This mapping

$$\{s_1, \cdots, s_{n_s}\} \rightarrow \mathbf{S}$$

can be defined in a variety of different ways. The procedure of designing this mapping has been heavily researched in recent years, with a good design producing codes that are easily encoded/decoded, provide high information rates and are resilient against decoding errors.

STBCs can be categorized into orthogonal space-time block codes (OSTBCs) and non-orthogonal space-time block codes (NOSTBCs). OSTBCs are designed such that the transmission matrices have orthogonal columns, allowing for linear-time decoding since the transmitted symbols are detected separately from each other [1][25]. In addition to low complexity decoding, OSTBCs provide full diversity gain. The shortcoming of orthogonal designs is that their existence with high rates (>1/2) is generally not well understood for an increasing number of transmit antennas. Moreover, the Hurwitz-Radon theorem (see [21, Section III.E]) shows that complex orthogonal designs cannot achieve full rate for greater than two transmit antennas [7][5][24]. NOSTBCs offer an effective way to increase the achievable rate by

relaxing orthogonality conditions while providing diversity gains for any number of antennas.

In the next few sections, OSTBC design will be introduced by first exploring Alamouti's two-branch transmit diversity scheme and then describing a generalized design by Tarokh *et al.* A popular form of NOSTBCs, called LDCs, will also be introduced as a high rate coding technique for any number of antennas.

2.5.1 Space-Time Orthogonal Block Codes

Before presenting Tarokh's generalized OSTBC structure, we investigate Alamouti's scheme to gain an understanding and appreciation for the simplicity of the setup.

2.5.1.1 Alamouti's Scheme

In his groundbreaking study in 1998 [1], Alamouti devised a simple two-branch transmit diversity scheme with one receive antenna. The setup was modeled as a dual to the MRRC technique, which employs one transmitter and two or more receive antennas, described in detail in [1][20].

Alamouti's two-branch transmit diversity scheme is shown in Fig. 2.5. During the first symbol period t_1, the symbols s_1 and s_2, which represent constellation points from any modulation scheme, are sent simultaneously from transmit antennas Tx_1 and Tx_2, respectively. In the next symbol period t_2, Tx_1 transmits $-s_2^*$ and Tx_2 transmits s_1^*, where $(\cdot)^*$ represent the complex conjugate.

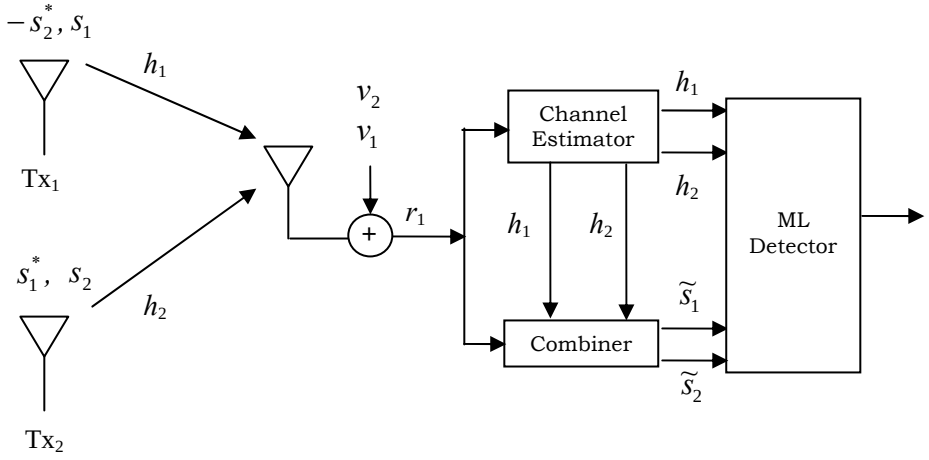

Figure 2.5 – Alamouti's two-branch transmit diversity scheme with one receiver

This simple orthogonal code can be represented in matrix form as

$$\mathbf{G}_2 = \begin{matrix} \\ t_1 \\ t_2 \end{matrix} \overbrace{\begin{matrix} \\ \mathrm{Tx}_1 \end{matrix} \quad \begin{matrix} \\ \mathrm{Tx}_2 \end{matrix}} \begin{matrix} \\ \left\{ \\ \\ \end{matrix} \begin{bmatrix} s_1 & s_2 \\ -s_2^* & s_1^* \end{bmatrix} \tag{2.13}$$

where the columns represent transmit antennas and the rows represent time. The orthogonality of (2.13) can be easily verified by multiplying the columns together

$$(s_1, -s_2^*) \cdot (s_2, s_1^*)^* = s_1 s_2^{\ *} + (-s_2^*)(s_1) = 0 .$$

Let $h_1(t)$ and $h_2(t)$ represent the path from Tx_1 and Tx_2 to the receiver, respectively. Assuming that channel fading is quasi-static, that is constant across two consecutive symbol transmissions, we have

$$h_1(t) = h_1(t+T) = h_1 = \alpha_1 e^{j\theta_1}$$
$$h_2(t) = h_2(t+T) = h_2 = \alpha_2 e^{j\theta_2} ,$$

where T is the symbol period. The corresponding received signals are

$$r_1 = r(t) = h_1 s_1 + h_2 s_2 + v_1$$
$$r_2 = r(t+T) = -h_1 s_2^* + h_2 s_1^* + v_2 ,$$

where r_1 and r_2 are the received signals and v_1 and v_2 are the additive Gaussian noise terms across the channel at symbol periods 1 and 2, respectively.

Once combined, the received signals are

$$\tilde{s}_1 = h_1^* r_1 + h_2 r_2^* = (\alpha_1^2 + \alpha_2^2) s_1 + h_1^* v_1 + h_2 v_2^*$$
$$\tilde{s}_2 = h_2^* r_1 - h_1 r_2^* = (\alpha_1^2 + \alpha_2^2) s_2 - h_1 v_2^* + h_2^* v_1$$

and are sent to the ML detector which then minimizes the decision metric

$$\left| r_1 - h_1 s_1 - h_2 s_2 \right|^2 + \left| r_2 + h_1 s_2^* - h_2 s_1^* \right|^2$$

over all possible pairs s_1 and s_2. This can be expanded and simplified to have two separate minimization expressions. The minimization expression to detect s_1 is

$$\left|r_1 h_1^* - r_2^* h_2 - s_1\right|^2 + (\alpha_1^2 + \alpha_2^2 - 1)\left|s_1\right|^2 \tag{2.14}$$

and the minimization expression to detect s_2 is

$$\left|r_1 h_2^* - r_2^* h_1 - s_2\right|^2 + (\alpha_1^2 + \alpha_2^2 - 1)\left|s_2\right|^2 . \tag{2.15}$$

Now defining $d^2(x,y)$ such that

$$d^2(x,y) = (x-y)(x^* - y^*) = \left|x-y\right|^2$$

the decision rule for each combined signal $\tilde{s}_j$ can be expressed as below, where s_i is chosen if and only if (iff)

$$(\alpha_1^2 + \alpha_2^2 - 1)\left|s_i\right|^2 + d^2(\tilde{s}_j, s_i) \le (\alpha_1^2 + \alpha_2^2 - 1)\left|s_k\right|^2 + d^2(\tilde{s}_j, s_k), \quad \forall k \ne i .$$

When using a PSK modulation, with equal energy constellations, the above inequality simplifies to

$$d^2(\tilde{s}_j, s_i) \le d^2(\tilde{s}_j, s_k), \quad \forall k \ne i .$$

Alamouti went on to extend his two transmit and one receive antenna scheme to $n_R > 1$ receive antennas. The resulting diversity order of the two-branch transmit diversity scheme with two receivers was shown to be equivalent to a four-branch MRRC scheme [1]. In general, this method provides a diversity order of $2n_R$, which is maximal since there are $n_T = 2$ transmit antennas.

2.5.1.2 Generalized Complex Orthogonal OSTBCs

Tarokh *et al.* [25] generalized Alamouti's scheme above to an arbitrary number of transmit antennas and presented design guidelines for real and complex-valued OSTBCs. These codes require no CSI at the transmitter, achieve ML decoding through linear processing at the receiver and exhibit maximum diversity gain. For real constellations (such as PAM), they are known to provide the maximum theoretical transmission rate. For complex constellations (such as PSK and QAM), OSTBCs can be constructed for $n_T > 2$ transmit antennas while providing full diversity and half of the maximum theoretical rate.

For brevity, this section will focus on complex orthogonal designs, though much of the discussion is analogous to the real orthogonal case. In fact, it is shown in [25] that a complex orthogonal design of size n_T determines a real orthogonal design of size $2n_T$ and, as a corollary square, complex orthogonal designs only exist for $n_T = 2$ or 4, since their real counterparts only exist for $n_T = 2, 4$ and 8 (see [22, Section V.C]). Furthermore, the authors find that complex orthogonal designs with full rate can only exist for $n_T = 2$ by proving that no such design exists for the case of $n_T = 4$.

A general complex OSTBC of size n_T can be represented by a $T \times n_T$ matrix $\mathbf{G}_k$ which transmits k data symbols from

$$0, \pm s_0, \pm s_0^*, \pm s_1, \pm s_1^*, \cdots, \pm s_k, \pm s_k^*$$

or their product with $j = \sqrt{-1}$. If we satisfy the condition that $\mathbf{G}_k^{\mathrm{t}} \mathbf{G}_k = \mathbf{D}_k$, where $\mathbf{D}_k$ is a diagonal matrix with $(i,i)^{\text{th}}$ diagonal entry of the form

$$l_0^i |s_0|^2 + l_1^i |s_1|^2 + \cdots + l_k^i |s_k|^2$$

such that the coefficients $l_0^i, l_1^i, \ldots, l_k^i > 0$, then $\mathbf{G}_k$ is said to be a generalized OSTBC with size n_T and rate $R = k/T \log_2 M$ bits per channel use, where M is the constellation size.

The existence of high-rate complex orthogonal designs is not well understood. A complex orthogonal design with full rate can only be found for the case where $n_T = 2$, which is exactly Alamouti's $\mathbf{G}_2$ code in (2.13). Tarokh *et al.* produced generalized complex designs with rate 1/2 ($\mathbf{G}_3$ and $\mathbf{G}_4$ below) and sporadic codes with rate 3/4 ($\mathbf{H}_3$ and $\mathbf{H}_4$ below). Recent work by Su *et al.* [22] produced generalized complex OSTBC design for 5 and 6 transmit antennas with rate 7/11 and 3/5 while Kan *et al.* [15] found an OSTBC with rate 5/8 for eight transmit antennas.

Rate 1/2 OSTBCs for three transmit antennas ($\mathbf{G}_3$) and four transmit antennas ($\mathbf{G}_4$) :

$$\mathbf{G}_3 = \begin{bmatrix} s_1 & s_2 & s_3 \\ -s_2 & s_1 & -s_4 \\ -s_3 & s_4 & s_1 \\ -s_4 & -s_3 & s_2 \\ s_1^* & s_2^* & s_3^* \\ -s_2^* & s_1^* & -s_4^* \\ -s_3^* & s_4^* & s_1^* \\ -s_4^* & -s_3^* & s_2^* \end{bmatrix},$$

$$\mathbf{G}_4 = \begin{bmatrix} s_1 & s_2 & s_3 & s_4 \\ -s_2 & s_1 & -s_4 & s_3 \\ -s_3 & s_4 & s_1 & -s_2 \\ -s_4 & -s_3 & s_2 & s_1 \\ s_1^* & s_2^* & s_3^* & s_4^* \\ -s_2^* & s_1^* & -s_4^* & s_3^* \\ -s_3^* & s_4^* & s_1^* & -s_2^* \\ -s_4^* & -s_3^* & s_2^* & s_1^* \end{bmatrix}.$$

Rate 3/4 OSTBCs for three transmit antennas ($\mathbf{H}_3$) and four transmit antennas ($\mathbf{H}_4$):

$$\mathbf{H}_3 = \begin{bmatrix} s_1 & s_2 & \frac{s_3}{\sqrt{2}} \\ -s_2^* & s_1^* & \frac{s_3}{\sqrt{2}} \\ \frac{s_3^*}{\sqrt{2}} & \frac{s_3^*}{\sqrt{2}} & \frac{-s_1 - s_1^* + s_2 - s_2^*}{2} \\ \frac{s_3^*}{\sqrt{2}} & -\frac{s_3^*}{\sqrt{2}} & \frac{s_2 + s_2^* + s_1 - s_1^*}{2} \end{bmatrix},$$

$$\mathbf{H}_4 = \begin{bmatrix} s_1 & s_2 & \frac{s_3}{\sqrt{2}} & \frac{s_3}{\sqrt{2}} \\ -s_2^* & s_1^* & \frac{s_3}{\sqrt{2}} & -\frac{s_3}{\sqrt{2}} \\ \frac{s_3^*}{\sqrt{2}} & \frac{s_3^*}{\sqrt{2}} & \frac{-s_1 - s_1^* + s_2 - s_2^*}{2} & \frac{-s_2 + s_2^* + s_1 - s_1^*}{2} \\ \frac{s_3^*}{\sqrt{2}} & -\frac{s_3^*}{\sqrt{2}} & \frac{s_2 + s_2^* + s_1 - s_1^*}{2} & \frac{-s_1 - s_1^* - s_2 + s_2^*}{2} \end{bmatrix}.$$

2.5.2 Linear Space-Time Block Codes

For high data rates and a large number of transmit antennas, STTCs and OSTBCs suffer from complexity and/or performance shortcomings. In STTCs, the number of trellis states grows exponentially with the number of transmit antennas [24] and finding high rate (>1/2) OSTBCs for an arbitrary number of transmit antennas is a daunting problem.

Hassibi *et al.* [11] present a new type of non-orthogonal linear-STBC called linear dispersion codes, since they work by dividing the data into substreams that are dispersed in linear combinations over space and time. These LDCs provide coding gain and diversity gain while maintaining relatively simple decoding for an arbitrary number of transmit and receive antennas. Heath *et al.* later proposed an LDC design guideline which sought optimality in both the ergodic capacity sense and the diversity gain sense in [12]. In this work we utilize the framework of the LDC and not the design conditions. Therefore, we restrict our discussion of LDCs to the findings of the pioneering paper of Hassibi *et al.* [11].

Encoding

For a system with n_T transmit antennas, n_R receive antennas and a symbol period T, the $T \times n_T$ transmitter matrix $\mathbf{S}$ can be written as

$$\mathbf{S} = \sum_{q=1}^{Q} \left(\alpha_q A_q + j\beta_q B_q \right) , \tag{2.16}$$

where the data is broken into Q substreams and the real scalars $\{\alpha_q, \beta_q\}$ are determined by $s_1, \cdots, s_q$, which are complex symbols chosen from an arbitrary constellation of size M and expressed as

$$s_q = \alpha_q + j\beta_q , \quad q = 1, \cdots, Q . \tag{2.17}$$

These codes have a rate of $R = {}^{Q}\!/_{T} \log_2 M$ bits per channel use.

The choices for the dispersion matrices $\{A_q, B_q\}$ and Q are critical factors in designing LDCs. The authors propose an information-theoretic approach to choosing these parameters such that the mutual information between the transmitted signals and received signals is maximized.

Decoding

Consider the following block equation for the system:

$$\begin{aligned} \mathbf{R} &= \sqrt{\frac{\gamma_s}{n_T}} \mathbf{S} \cdot \mathbf{H} + \mathbf{V} \\ &= \sqrt{\frac{\gamma_s}{n_T}} \sum_{q=1}^{Q} \left(\alpha_q A_q + j\beta_q B_q \right) \cdot \mathbf{H} + \mathbf{V} , \end{aligned} \tag{2.18}$$

where γ_s is the CSNR at each receive antenna, $\mathbf{R}$ is the received matrix, $\mathbf{V}$ is the noise matrix containing the Gaussian noise at each receive antenna, $\mathbf{H}$ is the channel gain matrix representing the path between transmit antenna i and receive antenna j for $i = 1, \ldots, n_T$ and $j = 1, \ldots, n_R$.

The receive matrix $\mathbf{R}$ can be decomposed into real and imaginary parts to get

$$\begin{aligned}\mathbf{R} &= \Re\{\mathbf{R}\} + j\Im\{\mathbf{R}\} \\ &= \sqrt{\frac{\gamma_s}{n_T}} \sum_{q=1}^{Q} \left[\alpha_q \left(\Re\{A_q\} + j\Im\{A_q\}\right) + j\beta_q \left(\Re\{B_q\} + j\Im\{B_q\}\right)\right] \\ &\qquad \times \left(\Re\{\mathbf{H}\} + j\Im\{\mathbf{H}\}\right) + \left(\Re\{\mathbf{V}\} + j\Im\{\mathbf{V}\}\right).\end{aligned}$$

Separating the real and imaginary parts, we get

$$\begin{aligned}\Re\{\mathbf{R}\} = \sqrt{\frac{\gamma_s}{n_T}} \sum_{q=1}^{Q} \Big[&\alpha_q \left(\Re\{A_q\}\Re\{\mathbf{H}\} - \Im\{A_q\}\Im\{\mathbf{H}\}\right) \\ &+ \beta_q \left(-\Im\{B_q\}\Re\{\mathbf{H}\} - \Re\{B_q\}\Im\{\mathbf{H}\}\right)\Big] + \Re\{\mathbf{V}\},\end{aligned}$$

$$\begin{aligned}\Im\{\mathbf{R}\} = \sqrt{\frac{\gamma_s}{n_T}} \sum_{q=1}^{Q} \Big[&\alpha_q \left(\Im\{A_q\}\Re\{\mathbf{H}\} + \Re\{A_q\}\Im\{\mathbf{H}\}\right) \\ &+ \beta_q \left(\Re\{B_q\}\Re\{\mathbf{H}\} - \Im\{B_q\}\Im\{\mathbf{H}\}\right)\Big] + \Im\{\mathbf{V}\}.\end{aligned}$$

Letting $\Re(r_j), \Im(r_j), \Re(h_j), \Im(h_j), \Re(v_j)$ and $\Im(v_j)$ represent the j^{th} columns of $\Re(\mathbf{R}), \Im(\mathbf{R}), \Re(\mathbf{H}), \Im(\mathbf{H}), \Re(\mathbf{V})$ and $\Im(\mathbf{V})$, respectively, we define

$$\begin{aligned}\mathcal{A}_q &= \begin{bmatrix} \Re\{A_q\} & -\Im\{A_q\} \\ \Im\{A_q\} & \Re\{A_q\} \end{bmatrix}, \\ \mathcal{B}_q &= \begin{bmatrix} -\Im\{B_q\} & -\Re\{B_q\} \\ \Re\{B_q\} & -\Im\{B_q\} \end{bmatrix}, \\ \underline{h}_j &= \begin{bmatrix} \Re\{h_j\} \\ \Im\{h_j\} \end{bmatrix},\end{aligned}$$

for $q = 1,\ldots,Q$ and $j = 1,\ldots,n_R$, where $\underline{h}_j$ has independent $\mathcal{CN}\left(0, \frac{1}{2}\right)$ entries.

With the above definitions, we rewrite the channel matrix as the $2n_R T \times 2Q$ matrix:

$$\mathcal{H} = \begin{bmatrix} \mathcal{A}_1 \underline{h}_1 & \mathcal{B}_1 \underline{h}_1 & \cdots & \mathcal{A}_Q \underline{h}_1 & \mathcal{B}_Q \underline{h}_1 \\ \vdots & \vdots & \ddots & \vdots & \vdots \\ \mathcal{A}_1 \underline{h}_{n_R} & \mathcal{B}_1 \underline{h}_{n_R} & \cdots & \mathcal{A}_Q \underline{h}_{n_R} & \mathcal{B}_Q \underline{h}_{n_R} \end{bmatrix} , \tag{2.19}$$

which is known to the receiver since the original **H** and the dispersion matrices $\{A_q, B_q\}$ are all known. The definition in (2.19) allows us to rewrite the entire system, in terms of a combined $\Re(\mathbf{R})$ and $\Im(\mathbf{R})$, as

$$\underbrace{\begin{bmatrix} \Re\{r_1\} \\ \Im\{r_1\} \\ \vdots \\ \Re\{r_{n_R}\} \\ \Im\{r_{n_R}\} \end{bmatrix}}_{r} = \sqrt{\frac{\gamma_s}{n_T}} \mathcal{H} \cdot \underbrace{\begin{bmatrix} \alpha_1 \\ \beta_1 \\ \vdots \\ \alpha_Q \\ \beta_Q \end{bmatrix}}_{s} + \underbrace{\begin{bmatrix} \Re\{v_1\} \\ \Im\{v_1\} \\ \vdots \\ \Re\{v_{n_R}\} \\ \Im\{v_{n_R}\} \end{bmatrix}}_{v} , \tag{2.20}$$

giving the linear input vector s and output vector r relation

$$r = \sqrt{\frac{\gamma_s}{n_T}} \mathcal{H} \cdot s + v \quad . \tag{2.21}$$

The system described above will have a solution as long as we satisfy the condition in $\mathcal{H}$ that $2Q \le 2n_R T \Leftrightarrow Q \le n_R T$. In choosing a value for Q, the authors make the following argument. The larger the value of Q, the larger the mutual information between the input (s) and the output (r), since the matrix **S** will have more degrees of freedom. However, the smaller the value of Q, the stronger the effect of coding becomes since the system of

equations in (2.20) becomes over-determined. In practice, it is suitable to take

$$Q = \min(n_T, n_R) \cdot T$$

since this typically maximizes the input-output mutual information while providing coding gain [11].

Now that Q has been determined the question remains as to how the dispersion matrices $\{A_q, B_q\}$ are to be defined. True to their information-theoretic approach, the authors choose the dispersion matrices via an optimization of the system capacity

$$C_{\mathrm{LD}}(\gamma_s, T, n_T, n_R) = \max_{A_q, B_q, q=1,\ldots,Q} \frac{1}{2T} \mathrm{E}\left[\log\det\left(I_{2n_R \cdot T} + \frac{\gamma_s}{n_T} \mathcal{H}\mathcal{H}^* \right) \right], \tag{2.22}$$

where $\mathcal{H}$ is given in (2.19). In general, there is no closed-form solution to (2.22) for arbitrary T, n_T and n_R.

In addition to the optimization above, to satisfy the normalization condition

$$\mathrm{E}\left[\mathrm{tr}\left(\mathbf{S}\mathbf{S}^*\right)\right] = n_T \cdot T, \tag{2.23}$$

$\{A_q, B_q\}$ are subject to one of the following normalization constraints

(i) $$\sum_{q=1}^{Q} \left[\mathrm{tr}\left(A_q^* A_q\right) + \mathrm{tr}\left(B_q^* B_q\right) \right] = 2n_T \cdot T, \tag{2.24}$$

(ii) $$\mathrm{tr}\left(A_q^* A_q\right) = \mathrm{tr}\left(B_q^* B_q\right) = \frac{n_T \cdot T}{Q}, \tag{2.25}$$

(iii) $$A_q^* A_q = B_q^* B_q = \frac{T}{Q} \cdot \mathbf{I}_{n_T}, \tag{2.26}$$

for $q = 1,...,Q$, where I_{n_T} is the $n_T \times n_T$ identity matrix. Note that these constraints get progressively more strict in ensuring (2.23) by forcing the symbols α_q and β_q to have equal energy over space and time resulting in higher coding gains at the expense of smaller mutual information results.

To demonstrate the simplicity of the LDC structure, consider the following representation of Alamouti's $\mathbf{G}_2$ code. For $Q = T = n_T = 2$ and $n_R = 1$, the set of dispersion matrices representing (2.13) are

$$A_0 = \begin{bmatrix} 1 & 0 \\ 0 & 1 \end{bmatrix}, \quad A_1 = \begin{bmatrix} 0 & 1 \\ -1 & 0 \end{bmatrix},$$
$$B_0 = \begin{bmatrix} 1 & 0 \\ 0 & -1 \end{bmatrix}, \quad B_1 = \begin{bmatrix} 0 & 1 \\ 1 & 0 \end{bmatrix}.$$

This representation of Alamouti's code will be used to initialize and compare our newly formed linear-STBCs in Chapter 3.

2.6 Complexity

In designing STBCs, there exists a tradeoff between information rate and decoding complexity. Knowing that OSTBCs cannot provide full-rate codes for greater than two transmit antennas, whereas NOSTBCs can do so for any number of antennas, it is important to assess the cost in terms of decoding complexity associated with abandoning the orthogonal structure.

Consider a general STBC which transmits k information symbols $s_1,...,s_k$ per block, chosen from M constellation points. For OSTBCs, the ML detector can separate the decoding decision for each individual transmitted symbol s_i, as demonstrated in the two-branch Alamouti setup in 2.5.1.1 with equations (2.14) and (2.15). Thus, decoding is done in linear time, requiring kM computations. The Alamouti $\mathbf{G}_2$ code transmits 2 symbols at a time, hence $k = 2$, giving a decoding complexity of $2M$.

In contrast, for NOSTBCs the ML decoder cannot separate the detecting decision by individual symbols. Instead it detects entire codewords (or blocks) at a time. This results in exponential decoding complexity, since the ML detector requires M^k computations.

Clearly there is a large complexity difference between the two code design schemes and one must take into consideration the advantages and disadvantages of OSTBC and NOSTBC designs and their system requirements in choosing a suitable coding scheme.

2.7 Pairwise Error Probability

The notion of pairwise error probability is a fundamental measure of the error performance of STCs. The codeword PEP, denoted by $P(\mathbf{S} \to \hat{\mathbf{S}})$,

expresses the probability of erroneously detecting the codeword $\hat{\mathbf{S}}$ when in fact $\mathbf{S}$ was transmitted. Behnamfar presents a derivation for the codeword PEP for arbitrary STBCs in [2], which is also derived by Lu *et al.* in [17].

It can be shown [23] that the codeword PEP can be expressed as

$$P\left(\mathbf{S} \to \hat{\mathbf{S}}\right) = \mathrm{E}_{\Delta^2_{\mathbf{S},\hat{\mathbf{S}}}}\left[Q\left(\sqrt{\frac{1}{2}\Delta^2_{\mathbf{S},\hat{\mathbf{S}}}} \right) \right] \tag{2.27}$$

where $Q(\cdot)$ is the Gaussian Q-function and $\Delta^2_{\mathbf{S},\hat{\mathbf{S}}}$ is the squared-distance between a pair of channel-faded transmitted codewords $\mathbf{S}$ and $\hat{\mathbf{S}}$ can be expressed as

$$\begin{aligned} \Delta^2_{\mathbf{S},\hat{\mathbf{S}}} &= \frac{\gamma_s}{n_T} \sum_{t=1}^{T} \sum_{j=1}^{n_R} \left| \sum_{i=1}^{n_T} h_{j,i} d_{i,t} \right|^2 \\ &= \frac{\gamma_s}{n_T} \sum_{j=1}^{n_R} \boldsymbol{h}_j^{\mathrm{t}} \mathbf{U}^{\mathrm{T}} \boldsymbol{h}_j , \end{aligned} \tag{2.28}$$

where we use our definition of $\mathbf{U}$ from above (2.9), that is

$$\mathbf{U} = \left\lfloor u_{k,i} = \sum\nolimits_t d_{i,t} d^*_{k,t} \right\rfloor$$

for $1 \le i,k \le n_T$ and where $d_{i,t} = s^i_t - \hat{s}^i_t$ and $\boldsymbol{h}_j = \left[h_{j,1}\, h_{j,2} \cdots h_{j,n_T} \right]^{\mathrm{T}}$ is the transpose of the j^{th} row of the channel matrix $\mathbf{H}$. Since $\mathbf{U}$ is Hermitian ($\mathbf{U}^{\mathrm{t}} = \mathbf{U}$) and non-negative definite, we can be decompose it into $\mathbf{U} = \mathbf{Y}^{\mathrm{t}}\mathbf{D}\mathbf{Y}$, where $\mathbf{D}$ is a non-negative definite diagonal matrix having the real-valued eigenvalues of $\mathbf{U}$ on its main diagonal and $\mathbf{Y}$ is a unitary matrix, that is $\mathbf{Y}^{\mathrm{t}}\mathbf{Y} = \mathbf{I}_{n_T}$.

Replacing $\mathbf{U}$ with $\mathbf{Y}^{\mathrm{t}}\mathbf{D}\mathbf{Y}$ in (2.28) and multiplying by 1/2, we get

$$\begin{aligned}\frac{1}{2}\Delta^2_{\mathbf{S},\hat{\mathbf{S}}} &= \frac{\gamma_s}{2n_T}\sum_{j=1}^{n_R}\boldsymbol{h}_j^{\mathrm{t}}\cdot\mathbf{Y}^{\mathrm{t}}\mathbf{D}\mathbf{Y}\cdot\boldsymbol{h}_j \\ &= \frac{\gamma_s}{2n_T}\sum_{j=1}^{n_R}\mathbf{X}_j^{\mathrm{t}}\mathbf{D}\mathbf{X}_j \\ &= \sum_{j=1}^{n_R}\sum_{i=1}^{n_T}\frac{\gamma_s}{2n_T}\lambda_i\left|x_{j,i}\right|^2\end{aligned} \tag{2.29}$$

where $\mathbf{X}_j = \mathbf{Y}\cdot\boldsymbol{h}_j$ with i.i.d. $\mathcal{CN}(0,1)$ i^{th} element $x_{j,i}$ and $\lambda_i = \mathbf{D}_{i,i}$. The *moment generating function* (MGF) of $\frac{1}{2}\Delta^2_{\mathbf{S},\hat{\mathbf{S}}}$ is expressed as

$$\begin{aligned}\boldsymbol{\Phi}_{\frac{1}{2}\Delta^2_{\mathbf{S},\hat{\mathbf{S}}}}(-s) &= \prod_{i=1}^{n_T}\frac{1}{\left(1+\delta_i^2 s\right)^{n_R n_i}} \\ &= \sum_{i=1}^{n_T}\sum_{k=0}^{n_R n_i-1}\frac{\alpha_{k+1,i}}{\left(s+\delta_i^{-2}\right)^{k+1}}\end{aligned} \tag{2.30}$$

where $\delta_i^2 = \frac{\gamma_s\lambda_i}{2n_T}$, λ_i is the i^{th} non-zero eigenvalue of $\mathbf{U}$ with multiplicity n_i and $\alpha_{n_T n_i-k,i}$ is the residue of (2.30) and is expressed as

$$\alpha_{n_T n_i-k,i} = \frac{1}{k!}\left\{\frac{d^k}{ds^k}\left[\left(s+\delta_i^{-2}\right)^{n_T n_i}\boldsymbol{\Phi}_{\frac{1}{2}\Delta^2_{\mathbf{S},\hat{\mathbf{S}}}}(-s)\right]\right\}_{s=p_i}, k=0,\ldots,n_T n_i-1. \tag{2.31}$$

Taking the inverse Laplace transform of (2.30) we get

$$f_{\frac{1}{2}\Delta^2_{\mathbf{S},\hat{\mathbf{S}}}}(x) = \sum_{i=1}^{n_T}\sum_{k=0}^{n_R n_i-1}\frac{\alpha_{k+1,i}}{k!}x^k e^{-\delta_i^{-2}x}, \quad x\geq 0. \tag{2.32}$$

Now (2.32) is applied to the expectation (2.27) to get

$$P\left(\mathbf{S}\to\hat{\mathbf{S}}\right) = \sum_{i=1}^{n_T}\sum_{k=1}^{n_R n_i}\frac{\alpha_{k,i}}{(k-1)!}\int_0^\infty x^{k-1}e^{-\delta_i^{-2}x}Q\left(\sqrt{x}\right)dx, \tag{2.33}$$

which follows the form established in the orthogonal block code symbol PEP between symbol pair (s_i, s_j), shown in [2], and provides a solution for (2.33) of the form

$$P(\mathbf{S} \to \hat{\mathbf{S}}) = \sum_{i=1}^{n_T} \sum_{k=1}^{n_R n_i} \frac{\beta_{k,i}}{2} \left(1 - \frac{\delta_i}{\sqrt{\delta_i^2 + 2}} \sum_{j=0}^{k-1} \binom{2j}{j} \frac{1}{\left(2\delta_i^2 + 4\right)^j} \right) \tag{2.34}$$

where $\beta_{k,i} = \delta_i^{2k} \alpha_{k,i}$.

The codeword PEP expression in (2.34) forms the foundation of our error rate analysis, which is the basis of the new non-orthogonal linear-STBC design and analysis in Chapter 3.

Chapter 3

Design of Linear-NOSTBCs

3.1 Error Analysis

In our code design, we are interested in finding non-orthogonal, linear space-time block codes that have low error probabilities and high information rates. Specifically, we want to find codes that minimize the total frame error rate performance.

3.1.1 Frame Error Rate and Bit Error Rate

A frame error (or codeword error) occurs when a codeword $\mathbf{S}_u$ is transmitted over the channel and received as $\mathbf{S}_i$ by the ML decoder in (2.12), which is denoted by the event ε_{ui}. With all codewords being equally likely, the FER is expressed as [2]

$$\begin{aligned} \mathrm{FER} &= \mathrm{P}\left(\hat{\mathbf{S}} \neq \mathbf{S}\right) \\ &= \sum_{u=1}^{M} \mathrm{P}\left(\varepsilon \mid \mathbf{S}_u\right)\mathrm{P}\left(\mathbf{S}_u\right) \\ &= \frac{1}{M}\sum_{u=1}^{M} \mathrm{P}\left(\bigcup_{i\neq u} \varepsilon_{ui}\right), \end{aligned} \tag{3.1}$$

where there are M codewords in the codebook and $\mathrm{P}\left(\varepsilon \mid \mathbf{S}_u\right)$ is the probability of an error event given $\mathbf{S}_u$ was sent.

The bit error rate represents the statistical proportion of bits received in error. The BER is expressed as [2]

$$\mathrm{BER} = \frac{1}{M}\sum_{u=1}^{M} \mathrm{P}_b\left(u\right) \tag{3.2}$$

where

$$\begin{aligned} \mathrm{P}_b\left(u\right) &= \frac{1}{\log_2 M}\sum_{j=1}^{M} D_H\left(j,u\right)\cdot\mathrm{P}\left(\hat{\mathbf{S}} = \mathbf{S}_j \mid \mathbf{S} = \mathbf{S}_u\right) \\ &= \frac{1}{\log_2 M}\sum_{j=1}^{M} D_H\left(j,u\right)\left(1 - \mathrm{P}_u\left(\bigcup_{i\neq j} \varepsilon_{ji}\right)\right), \end{aligned} \tag{3.3}$$

where $m = \log_2 M$ is the number of data bits and $D_H\left(j,u\right)$ is the *Hamming distance* between the bits representing $\mathbf{S}_j$ and $\mathbf{S}_u$.

3.1.2 Union Bound

Both the FER expression in (3.1) and the BER expression in (3.2) rely on the calculation of the probability of a union of events. In practice, it is infeasible

to make this calculation and it is acceptable to use an upper or lower bound in its place.

The union bound is one such upper bound on the probability of a union which utilizes the basic probability inequality

$$\mathrm{P}\left(A_i \cup A_j\right) \leq \mathrm{P}\left(A_i\right) + \mathrm{P}\left(A_j\right).$$

Applying this to the probability of union seen in (3.1) and (3.2), we represent the union bound on the probability of a union of error events knowing that $\mathbf{S}_u$ was sent as

$$\mathrm{P}_u\left(\bigcup_{i \neq u} \varepsilon_{ui}\right) \leq \sum_{\substack{i=1 \\ i \neq u}}^{M} \mathrm{P}\left(\varepsilon_{ui}\right) \tag{3.4}$$

as shown in [28][19], where $\mathrm{P}\left(\varepsilon_{ui}\right)$ is the PEP between $\mathbf{S}_i$ and $\mathbf{S}_u$, which was derived in Section 2.7 and is expressed in (2.34).

Substituting (3.4) in (3.1), we get

$$\mathrm{FER} \leq \frac{1}{M} \sum_{u=1}^{M} \sum_{\substack{i=1 \\ i \neq u}}^{M} \mathrm{P}\left(\varepsilon_{ui}\right),$$

which agrees with the findings of [14, section 4.2.2]. The FER union upper bound expression in terms of the system parameters can now be expressed by substituting (2.34) above to get

$$\mathrm{FER}\left(M, \gamma_{\mathrm{s}}, n_T, n_R\right) \leq \frac{1}{M} \sum_{u=1}^{M} \sum_{\substack{i=1 \\ i \neq u}}^{M} \left[\sum_{y=1}^{n_T} \sum_{k=1}^{n_R n_y} \frac{\beta_{k,y}}{2} \left(1 - \frac{\delta_y}{\sqrt{\delta_y^2 + 2}} \sum_{j=0}^{k-1} \binom{2j}{j} \frac{1}{\left(2\delta_y^2 + 4\right)^j} \right) \right] \tag{3.5}$$

Equation (3.5) is the optimization expression in our design of new linear-STBCs as the dispersion matrices $\{A_q, B_q\}$ are iteratively perturbed to minimize this FER upper bound.

3.2 Linear-STBC Design

3.2.1 Overview

The LDCs by Hassibi *et al.* in Section 2.5.2 were designed to optimize the capacity of a multi-antenna system via a method which maximizes the mutual information between the input and output symbols [11]. In this study, we design our linear-STBCs to minimize the FER union upper bound in (3.5) via an iterative random search process of finding dispersion matrices $\{A_q, B_q\}$ which provide increasingly lower FER upper bounds. We note that the random search process is simple but far from optimal. For future extensions of this work, a more sophisticated search method such as simulated annealing or a gradient-based search would be more suitable in finding better dispersion matrices in less time.

All codes are designed for a system with $n_T = 2$, $T = 2$ and for a CSNR of 5 dB. The design process begins with an initialization for the dispersion matrices, $\{A_q, B_q\}$. In this work, we produce three different code

initialization scenarios with three different well-known codes: one with Alamouti's orthogonal $\mathbf{G}_2$ code, another with the V-BLAST code by Wolniansky *et al.* and a third with an LDC code presented by Hassibi *et al.* In each case, the formation of our codes follows an identical procedure, producing non-orthogonal STBCs of the form

$$\mathbf{G}_{\text{NEW}} = \begin{bmatrix} s_1 & s_2 \\ s_3 & s_4 \end{bmatrix}, \tag{3.6}$$

where the s_i are chosen from a BPSK constellation (Fig. 3.1(i)). Since $\mathbf{G}_{\text{NEW}}$ is designed with BPSK modulation, i.e. no complex component, all the B_i dispersion matrices for the new codes will be zero in all design cases, for $i = 1,\ldots,Q$.

Design with Alamouti-Initialization

For this design scenario, we initialize the new code dispersion matrices with Alamouti's $\mathbf{G}_2$ code, which is expressed in linear-STBC notation by the dispersion matrices

$$\begin{aligned} A_1 &= \begin{bmatrix} 1 & 0 \\ 0 & 1 \end{bmatrix}, \quad A_2 = \begin{bmatrix} 0 & 1 \\ -1 & 0 \end{bmatrix}, \\ B_1 &= \begin{bmatrix} 1 & 0 \\ 0 & -1 \end{bmatrix}, \quad B_2 = \begin{bmatrix} 0 & 1 \\ 1 & 0 \end{bmatrix}. \end{aligned} \tag{3.7}$$

For the case of 2×2 block codewords, Alamouti's design will transmit 2 symbols in 2 symbol periods, whereas the new code design will transmit 4 symbols in that time. In order to maintain the same transmission rate, the

design algorithm uses QPSK modulation (Fig. 3.1 (ii)) for Alamouti's code, compared with BPSK modulation for the new codes. This produces a rate of 4 bits per channel use (PCU) for both codes.

Figure 3.1 – (i) BPSK and (ii) QPSK constellations

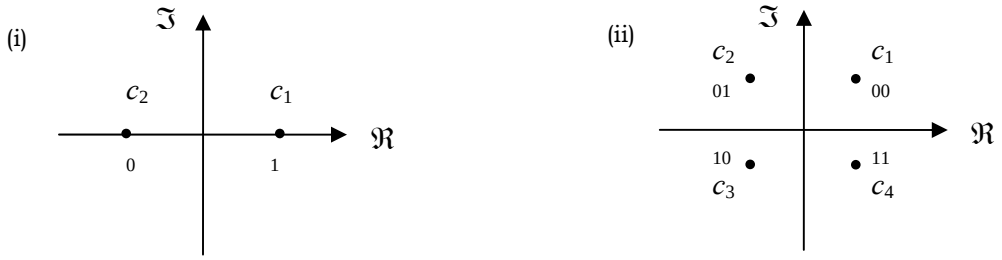

Design with V-BLAST-Initialization

The V-BLAST code structure has a similar form as our code in (3.6) with the major exception that the codewords follow a vertically layered encoding scheme and do not provide transmit diversity, since the input bit substreams are associated exclusively with one transmit antenna [27].

For this design scenario, we initialize the new code dispersion matrices with the linear-STBC representation of V-BLAST with dispersion matrices

$$A_1 = B_1 = \begin{bmatrix} 1 & 0 \\ 0 & 0 \end{bmatrix}, \quad A_2 = B_2 = \begin{bmatrix} 0 & 1 \\ 0 & 0 \end{bmatrix},$$
$$A_3 = B_3 = \begin{bmatrix} 0 & 0 \\ 1 & 0 \end{bmatrix}, \quad A_4 = B_4 = \begin{bmatrix} 0 & 0 \\ 0 & 1 \end{bmatrix}. \tag{3.8}$$

We use BPSK modulation for V-BLAST, thus B_i will be zero for $i = 1,\ldots,Q$.

Design with LDC-Initialization

Since our new code design is based on the LDC framework in [11], it is of interest to test whether our design technique can provide improved error rate performance compared to those presented by Hassibi *et al.*

A description of an LDC code is provided in [11, pp. 1813] where the dispersion matrices are formed via a transformation of the dispersion matrices that we defined in Chapter 2. For the $T = n_T = 2$ case, the new matrices, denoted as A'_i for $i = 1,...,Q$, are expressed as

$$\begin{aligned} A'_1 &= \frac{A_1 + A_4}{\sqrt{2}} = \begin{bmatrix} 1/\sqrt{2} & 0 \\ 0 & 1/\sqrt{2} \end{bmatrix}, \; A'_2 = \frac{A_2 + A_3}{\sqrt{2}} = \begin{bmatrix} 0 & 1/\sqrt{2} \\ 1/\sqrt{2} & 0 \end{bmatrix} \\ A'_3 &= \frac{A_1 - A_4}{\sqrt{2}} = \begin{bmatrix} 1/\sqrt{2} & 0 \\ 0 & -1/\sqrt{2} \end{bmatrix}, \; A'_4 = \frac{A_2 - A_3}{\sqrt{2}} = \begin{bmatrix} 0 & 1/\sqrt{2} \\ -1/\sqrt{2} & 0 \end{bmatrix}, \end{aligned} \tag{3.9}$$

with a similar set of transformations for B'_i. The authors take the A_i and B_i values from the V-BLAST code in (3.8) to form A'_i and B'_i in (3.9), for $i = 1,...,Q$. The code design is again modulated with a BPSK constellation.

3.2.2 Implementation

The design algorithm can be summarized as a five step process:

Step 1. Initialize A_i and B_i based on the desired starting code

Step 2. Find the FER union upper bound in (3.5) using the codewords formed by the normalized A_i and B_i, subject to constraint (2.25)

Step 3. If the new upper bound is lower than the previous best then save the dispersion matrices and the upper bound

Step 4. Perturb A_i and B_i

Step 5. Repeat steps 2 – 4 until you have 10^6 consecutive iterations with no FER upper bound improvement

The code design was implemented entirely in the *C*-programming language. The table below highlights the key functions used in the program to implement the iterative random search process.

Table 3.1 – Design implementation functions

Function Name	Description
temp_mtx()	Initializes the temporary A_i and B_i matrices
perturb_matrix()	Takes a matrix input and perturbs the individual values by via additive Gaussian noise
create_codeword()	Creates the new codebook based on the constellation points and the current versions of the A_i and B_i
eigen_U()	Takes in two matrices, $\Re\{\mathbf{D}\}$ and $\Im\{\mathbf{D}\}$, representing the real and imaginary parts of the matrix $\mathbf{D}$, and two eigenvalues of $\mathbf{D}$ in ascending order and produces the eigenvalues of $\mathbf{U} = \mathbf{D}\mathbf{D}^{\mathrm{t}}$
UBound()	This function performs the computations to produce the union upper bound in (3.5) using the PEP expression in (2.34). The inputs are the real and complex codewords matrices, the number of receive antennas, the CSNR, the number of transmit antennas and the codebook size.
main()	The main() program first performs all necessary initializations, including setting parameters like the CSNR, number of transmit/receive antennas, symbol period, codebook size and constellation size. The core feature of the main program is a

	for-loop in which the codewords are created using the current A_i and B_i and the union upper bound on the FER is calculated. If the new upper bound is better than the previously saved best, then the new code values are kept. Otherwise they are discarded. The main program also performs the normalization on A_i and B_i, subject to constraint (2.25), to ensure that the total transmit power remains constant as the matrices are perturbed.

The following flow chart diagram shows the various steps that the design program takes in producing improved code designs.

Figure 3.2 – Design program flow diagram

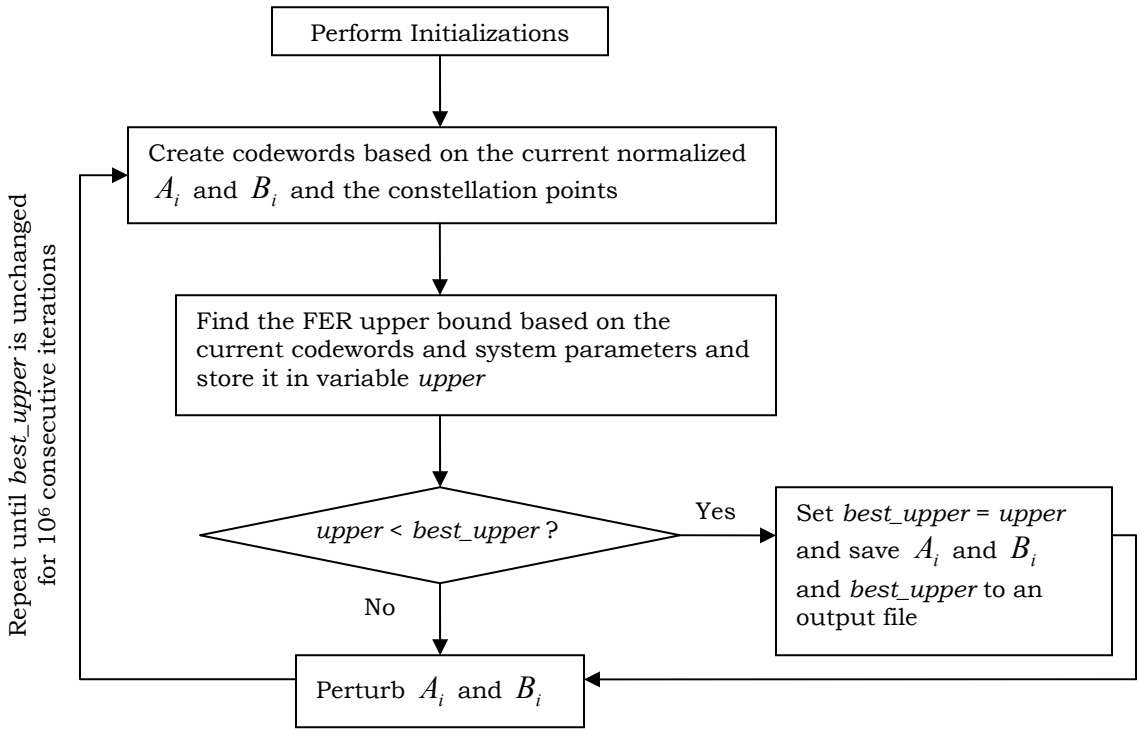

3.2.3 Design Results

Design Results with Alamouti-Initializaton

Table 3.2 shows the FER union upper bound results for the new code design $\mathbf{G}_{\text{NEW}}$ compared with Alamouti's $\mathbf{G}_2$ code for the case with 1, 2 and 4 receive antennas.

Table 3.2 – FER union upper bound results with Alamouti-initialization

	$n_R = 1$	$n_R = 2$	$n_R = 4$
Alamouti, $\mathbf{G}_2$	7.313696×10^{-1}	1.592608×10^{-1}	2.087142×10^{-2}
New code, $\mathbf{G}_{\text{NEW}}$	No Improvement	1.368865×10^{-1}	6.612724×10^{-3}

For the case of $n_R = 1$, the $\mathbf{G}_2$ upper bound is lower than the bounds found by the new code design algorithm. This result is not surprising since it was shown in [11] that the $\mathbf{G}_2$ code maximizes mutual information under the given system conditions with $n_T = 2$ and $n_R = 1$, which also has positive implications on error rate performance [11].

For the case of $n_R = 2$, a $\mathbf{G}_{\text{NEW}}$ code was found with a lower upper bound than the $\mathbf{G}_2$ code. The dispersion matrices which produced the upper bound in Table 3.2 are

$$
\begin{aligned}
A_1 &= \begin{bmatrix} -0.486790 & -0.562228 \\ 1.090112 & -0.508519 \end{bmatrix}, \\
A_2 &= \begin{bmatrix} -0.767843 & 0.725407 \\ 0.320311 & 0.884083 \end{bmatrix}, \\
A_3 &= \begin{bmatrix} 0.486523 & 1.034857 \\ 0.505240 & -0.661135 \end{bmatrix}, \\
A_4 &= \begin{bmatrix} -0.710130 & 0.540755 \\ -0.854115 & -0.688322 \end{bmatrix}.
\end{aligned}
\tag{3.10}
$$

Finally, for the case of $n_R = 4$, a significant improvement in the upper bound was found in $\mathbf{G}_{\text{NEW}}$ code with dispersion matrices

$$
\begin{aligned}
A_1 &= \begin{bmatrix} -0.153674 & 0.978861 \\ -0.776633 & -0.644249 \end{bmatrix}, \\
A_2 &= \begin{bmatrix} 0.868969 & -0.331196 \\ 0.170152 & -1.051785 \end{bmatrix}, \\
A_3 &= \begin{bmatrix} 1.100188 & 0.594767 \\ -0.167725 & 0.638520 \end{bmatrix}, \\
A_4 &= \begin{bmatrix} -0.099872 & 0.725076 \\ 1.159683 & -0.345582 \end{bmatrix}.
\end{aligned}
\tag{3.11}
$$

Design Results with V-BLAST-Initializaton

Table 3.3 shows the FER union upper bound results for the new code design $\mathbf{G}_{\text{NEW}}$ compared with V-BLAST for the case with 1, 2 and 4 receive antennas.

Table 3.3 – FER union upper bound results with V-BLAST-initialization

	$n_R = 1$	$n_R = 2$	$n_R = 4$
V-BLAST	1.535247×10^{0}	5.188582×10^{-1}	9.4444677×10^{-2}
New code, $\mathbf{G}_{\text{NEW}}$	1.116808×10^{0}	2.676792×10^{-1}	2.0017310×10^{-2}

For the case of $n_R = 1$, a $\mathbf{G}_{\text{NEW}}$ code is found with a lower FER union upper bound than the V-BLAST code. The dispersion matrices that produced this bound are

$$\begin{aligned} A_1 &= \begin{bmatrix} -0.363352 & -0.278428 \\ -0.416230 & 0.785625 \end{bmatrix}, \\ A_2 &= \begin{bmatrix} 0.278372 & -0.395207 \\ -0.715753 & -0.504002 \end{bmatrix}, \\ A_3 &= \begin{bmatrix} 0.816008 & 0.221152 \\ 0.459423 & 0.272310 \end{bmatrix}, \\ A_4 &= \begin{bmatrix} 0.584639 & -0.752010 \\ 0.248661 & 0.175630 \end{bmatrix}. \end{aligned} \tag{3.12}$$

For the case of $n_R = 2$, another $\mathbf{G}_{\text{NEW}}$ code was found with a lower upper bound than the V-BLAST code. The improvement in the upper bound was greater for this case than the case with 1 receive antenna. The dispersion matrices which produced the upper bound in Table 3.3 are

$$
\begin{aligned}
A_1 &= \begin{bmatrix} 0.543712 & 0.567503 \\ 0.527503 & -0.322580 \end{bmatrix}, \\
A_2 &= \begin{bmatrix} 0.425864 & 0.363339 \\ -0.766769 & 0.314150 \end{bmatrix}, \\
A_3 &= \begin{bmatrix} -0.313169 & 0.249101 \\ 0.197433 & 0.894927 \end{bmatrix}, \\
A_4 &= \begin{bmatrix} 0.754119 & -0.357025 \\ 0.266284 & 0.482629 \end{bmatrix}.
\end{aligned}
\tag{3.13}
$$

Finally, for the case of $n_R = 4$, an even greater improvement than the 2 receive antenna case was found in the upper bound from the $\mathbf{G}_{\text{NEW}}$ code with dispersion matrices

$$
\begin{aligned}
A_1 &= \begin{bmatrix} 0.355736 & -0.676318 \\ -0.412632 & -0.495763 \end{bmatrix}, \\
A_2 &= \begin{bmatrix} 0.803270 & 0.445861 \\ -0.161457 & 0.360413 \end{bmatrix}, \\
A_3 &= \begin{bmatrix} -0.532289 & -0.239878 \\ -0.554519 & 0.592989 \end{bmatrix}, \\
A_4 &= \begin{bmatrix} -0.065087 & 0.586357 \\ -0.679467 & -0.436203 \end{bmatrix}.
\end{aligned}
\tag{3.14}
$$

Design Results with LDC-Initializaton

Table 3.4 shows the FER union upper bound results for the new code design $\mathbf{G}_{\text{NEW}}$ compared with the LDC in (3.9) for the case with 1, 2 and 4 receive antennas.

Table 3.4 – FER union upper bound results with LDC-initialization

	$n_R = 1$	$n_R = 2$	$n_R = 4$
LDC	1.287384×10^{0}	3.610328×10^{-1}	5.391041×10^{-2}
New code, $\mathbf{G}_{\text{NEW}}$	1.110078×10^{0}	2.606916×10^{-1}	1.926679×10^{-2}

For the case of $n_R = 1$, a $\mathbf{G}_{\text{NEW}}$ code is found with a lower FER union upper bound than the LDC code. The dispersion matrices that produced this bound are

$$\begin{aligned} A_1 &= \begin{bmatrix} -0.313511 & -0.269378 \\ -0.284302 & 0.865054 \end{bmatrix}, \\ A_2 &= \begin{bmatrix} 0.178560 & 0.866510 \\ -0.448797 & 0.125928 \end{bmatrix}, \\ A_3 &= \begin{bmatrix} -0.256606 & 0.529601 \\ 0.752566 & 0.295500 \end{bmatrix}, \\ A_4 &= \begin{bmatrix} -0.683246 & 0.408703 \\ -0.315699 & -0.1516209 \end{bmatrix}. \end{aligned} \tag{3.15}$$

For the case of $n_R = 2$, another $\mathbf{G}_{\text{NEW}}$ code was found with a lower upper bound than the LDC code. Again, the improvement in the upper bound was greater for this case than the case with 1 receive antenna. The dispersion matrices which produced the upper bound in Table 3.4 are

$$
\begin{aligned}
A_1 &= \begin{bmatrix} -0.305120 & 0.221681 \\ 0.495505 & 0.782454 \end{bmatrix}, \\
A_2 &= \begin{bmatrix} -0.735799 & 0.387884 \\ -0.271442 & -0.484216 \end{bmatrix}, \\
A_3 &= \begin{bmatrix} -0.160018 & -0.554545 \\ -0.759056 & 0.301178 \end{bmatrix}, \\
A_4 &= \begin{bmatrix} 0.419005 & 0.743167 \\ -0.504240 & 0.133715 \end{bmatrix}.
\end{aligned}
\tag{3.16}
$$

Finally, for the case of $n_R = 4$, an even more significant improvement in the upper bound was found in the $\mathbf{G}_{\text{NEW}}$ code with dispersion matrices

$$
\begin{aligned}
A_1 &= \begin{bmatrix} -0.434715 & 0.694024 \\ 0.531583 & 0.216270 \end{bmatrix}, \\
A_2 &= \begin{bmatrix} -0.769450 & -0.378470 \\ -0.336463 & 0.389230 \end{bmatrix}, \\
A_3 &= \begin{bmatrix} 0.263345 & 0.413053 \\ -0.661579 & 0.567759 \end{bmatrix}, \\
A_4 &= \begin{bmatrix} -0.320807 & 0.291678 \\ -0.698364 & -0.569469 \end{bmatrix}.
\end{aligned}
\tag{3.17}
$$

The results in Tables 3.2, 3.3 and 3.4 indicate that the potential for FER upper bound improvement increases as the number of receive antennas does, regardless of which code we choose to initialize with. In the next chapter, these newly designed codes (3.10)-(3.17) will be tested in a simulation and their FER and BER performance will be compared with their respective initialization codes.

Chapter 4

Simulation Results & Discussion

4.1 Simulation Design

In order to validate the FER upper bounds found in the design chapter, shown in Tables 3.2-3.4, we test the dispersion matrices (3.10)-(3.17) via computer simulation. The simulation takes a set of dispersion matrices and, based on the chosen modulation scheme, produces an indexed set of codewords. For our case, the Alamouti code is designed with a QPSK modulation and all other codes ($\mathbf{G}_{NEW}$, V-BLAST and LDC) are designed with BPSK modulation.

Figure 4.1 shows the simulation process for a given set of dispersion matrices and constellation points. The MATLAB program performs 5×10^4 repetitions of a codeword transmission and detection method for each CSNR

in a specified range. Each time the transmitted codeword index does not match the ML detector index, the frame error counter is incremented. After 5×10^4 iterations for a particular CSNR, the FER for that CSNR is calculated by dividing the total frame errors by the total frames sent, i.e. 5×10^4.

Figure 4.1 – Simulation program flow diagram

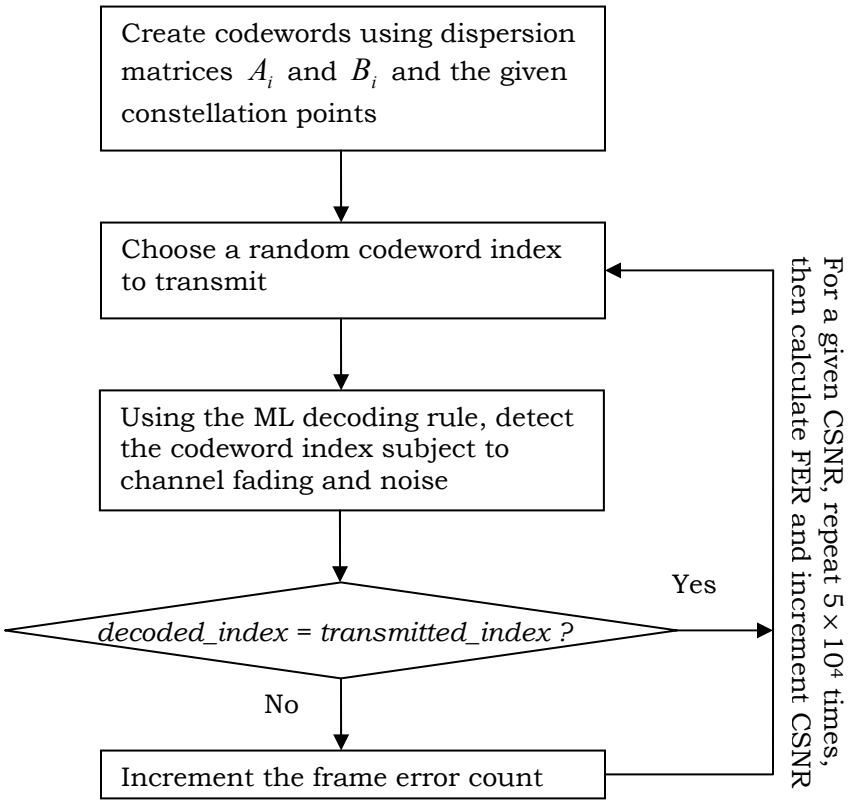

Similarly, to find the BER, the simulation keeps track of the bit representations of the codewords and finds the Hamming distance between the transmitted codeword and detected codeword. For each bit difference, a bit error counter is incremented and after 5×10^4 iterations the total bit error

count is divided by the total number of bits transmitted, that is 4 bits × 5×10^4 iterations = 2×10^5.

4.2 Simulation Results

Simulation Results for Alamouti-Initialization

Figure 4.2 shows the FER versus CSNR plot of the Alamouti $\mathbf{G}_2$ code and the $\mathbf{G}_{\text{NEW}}$ code in (3.10) with $n_R = 2$. We observe that for the range of CSNRs shown, the new code outperforms Alamouti's code with gains by upwards of 2.5 dB at a CSNR of 2.5 dB.

Figure 4.3 shows the BER versus CSNR for the same setup. Again we observe that the new code provides a gain upwards of 2.5 dB at a CSNR of 2.5 dB over the Alamouti code.

Figure 4.2 – FER for Alamouti-QPSK, New-BPSK for 2 Tx, 2 Rx

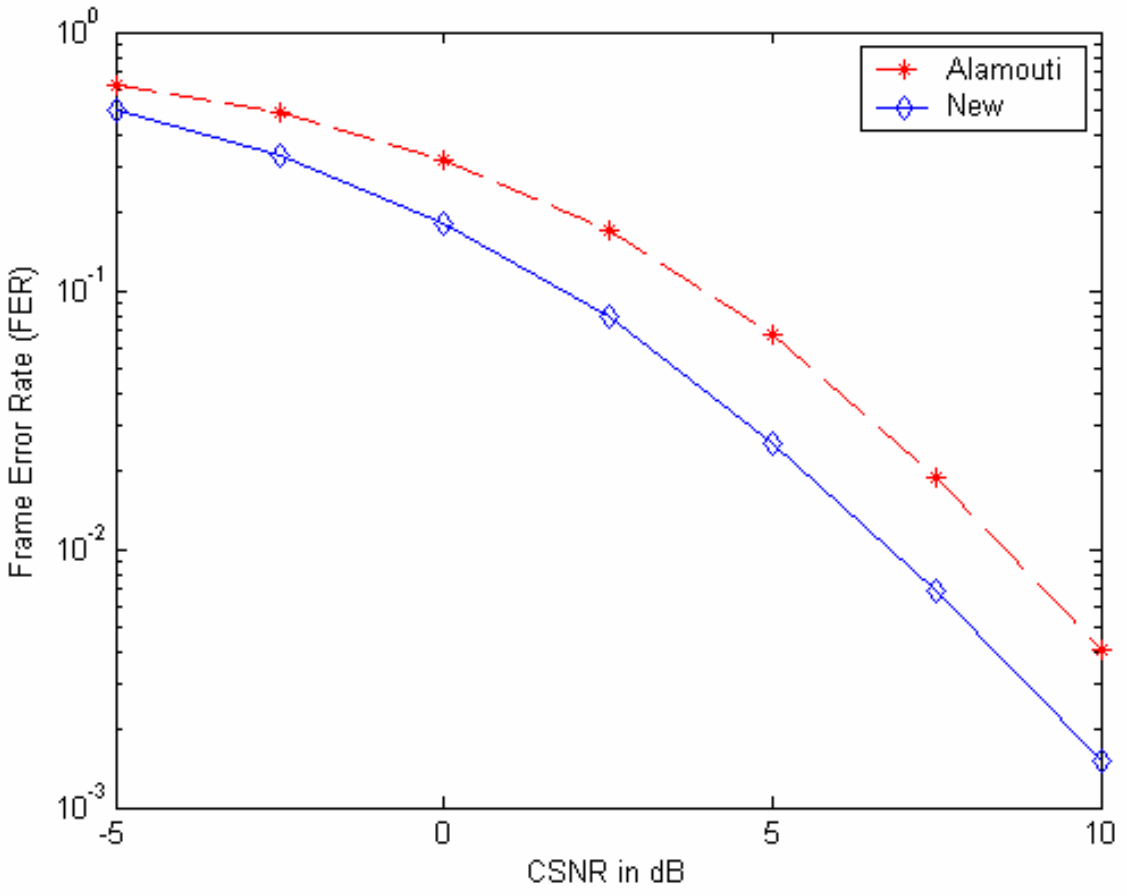

Figure 4.3 – BER for Alamouti-QPSK, New-BPSK for 2 Tx, 2 Rx

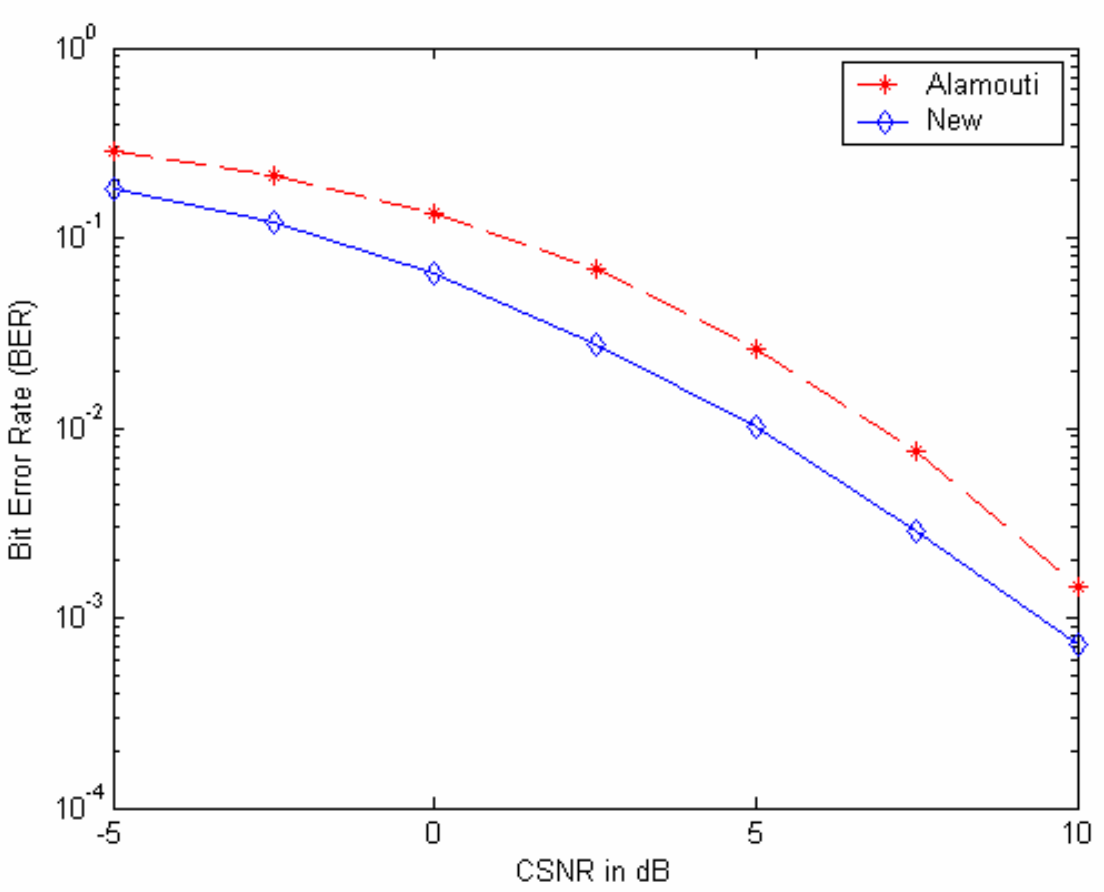

In Figure 4.4, the FER versus CSNR plot of the Alamouti $\mathbf{G}_2$ code and the $\mathbf{G}_{\text{NEW}}$ code design is shown with dispersion matrices shown in (3.11) for the case with $n_R = 4$. Here, the new code outperforms with gains upwards to 3 dB over Alamouti's code at a CSNR of 0 dB.

Figure 4.4 – FER for Alamouti-QPSK, New-BPSK for 2 Tx, 4 Rx

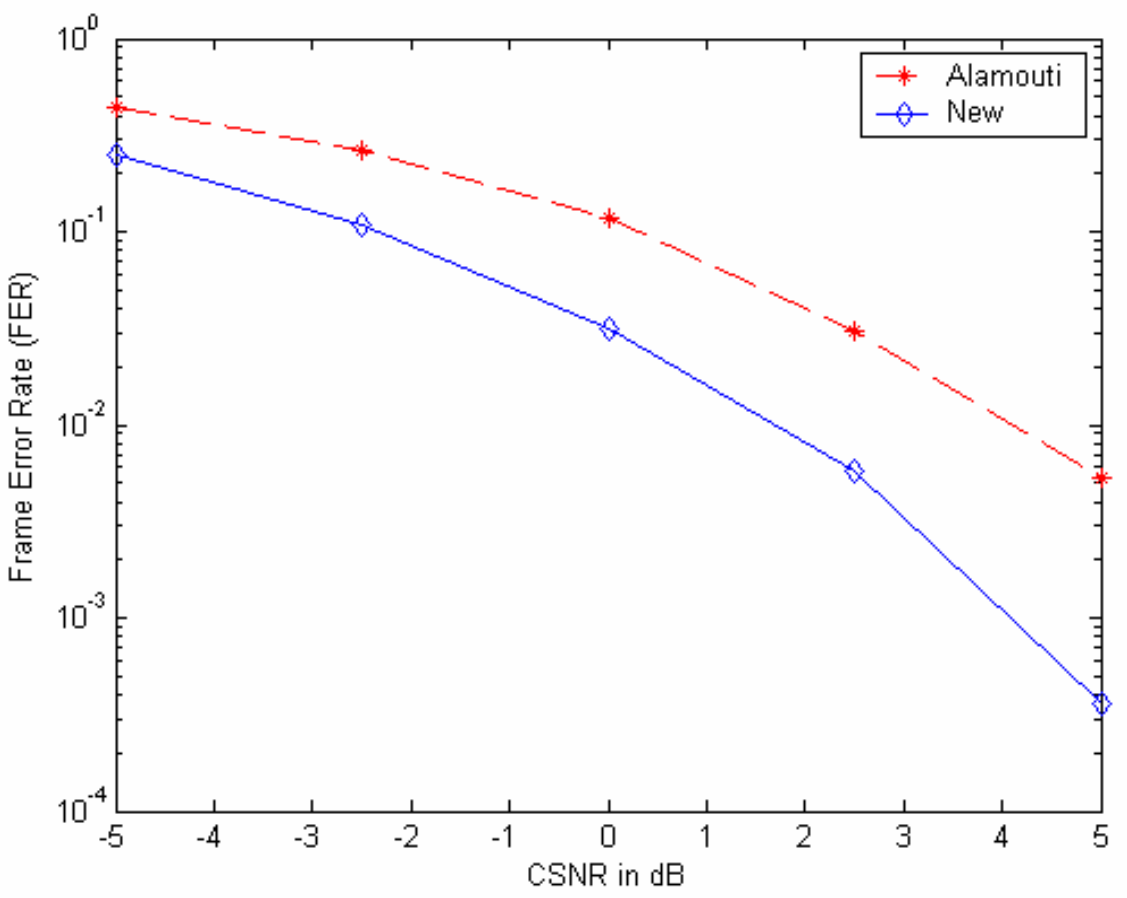

Figure 4.5 – BER for Alamouti-QPSK, New-BPSK for 2 Tx, 4 Rx

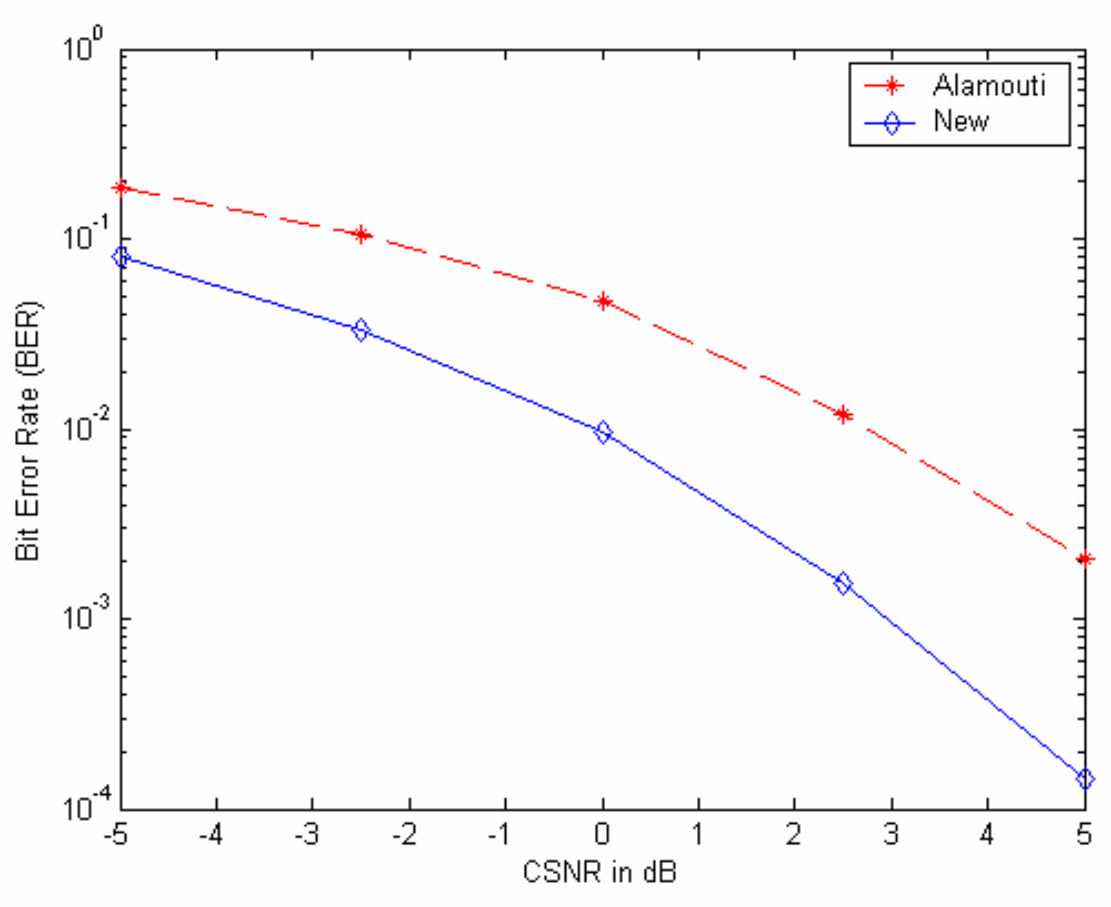

Figure 4.5 shows the BER versus CSNR for the same codes and where $n_R = 4$. Once again, the new code provides a gain upwards to 3 dB compared to the Alamouti code.

Simulation Results for V-BLAST-Initialization

Figures 4.6-4.11 show FER and BER plots for the new V-BLAST-initialized codes presented in (3.12), (3.13) and (3.14) with 1, 2 and 4 receive antennas, respectively, compared with the V-BLAST code in (3.8).

Figure 4.6 – FER for V-BLAST-BPSK, New-BPSK for 2 Tx, 1 Rx

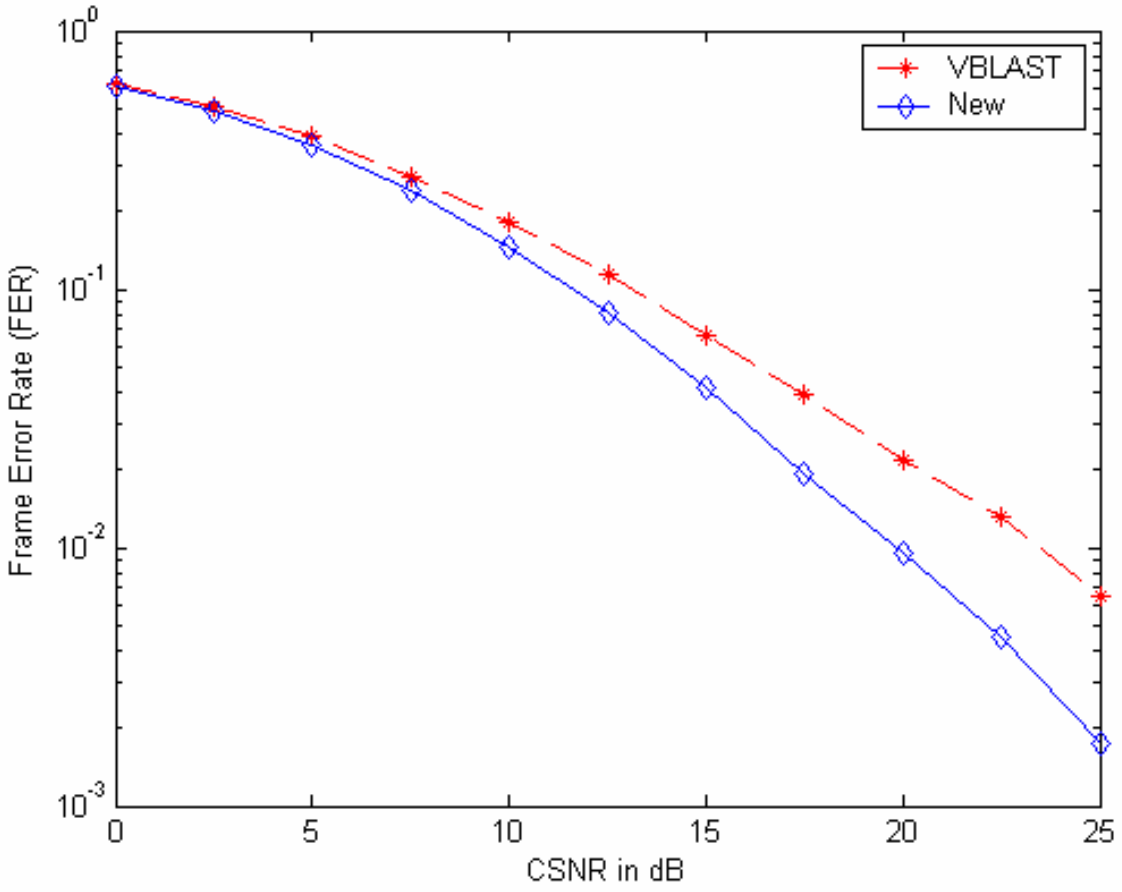

Figure 4.7 – BER for V-BLAST-BPSK, New-BPSK for 2 Tx, 1 Rx

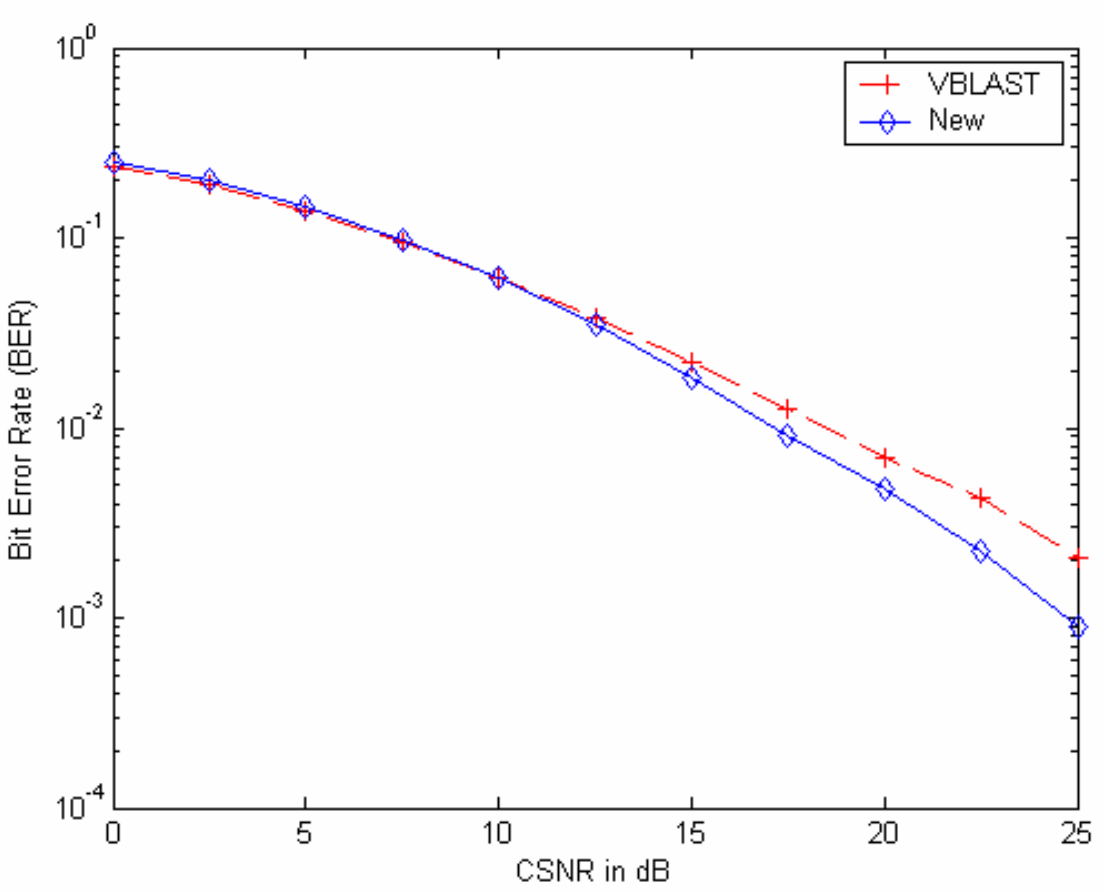

Figure 4.8 – FER for V-BLAST-BPSK, New-BPSK for 2 Tx, 2 Rx

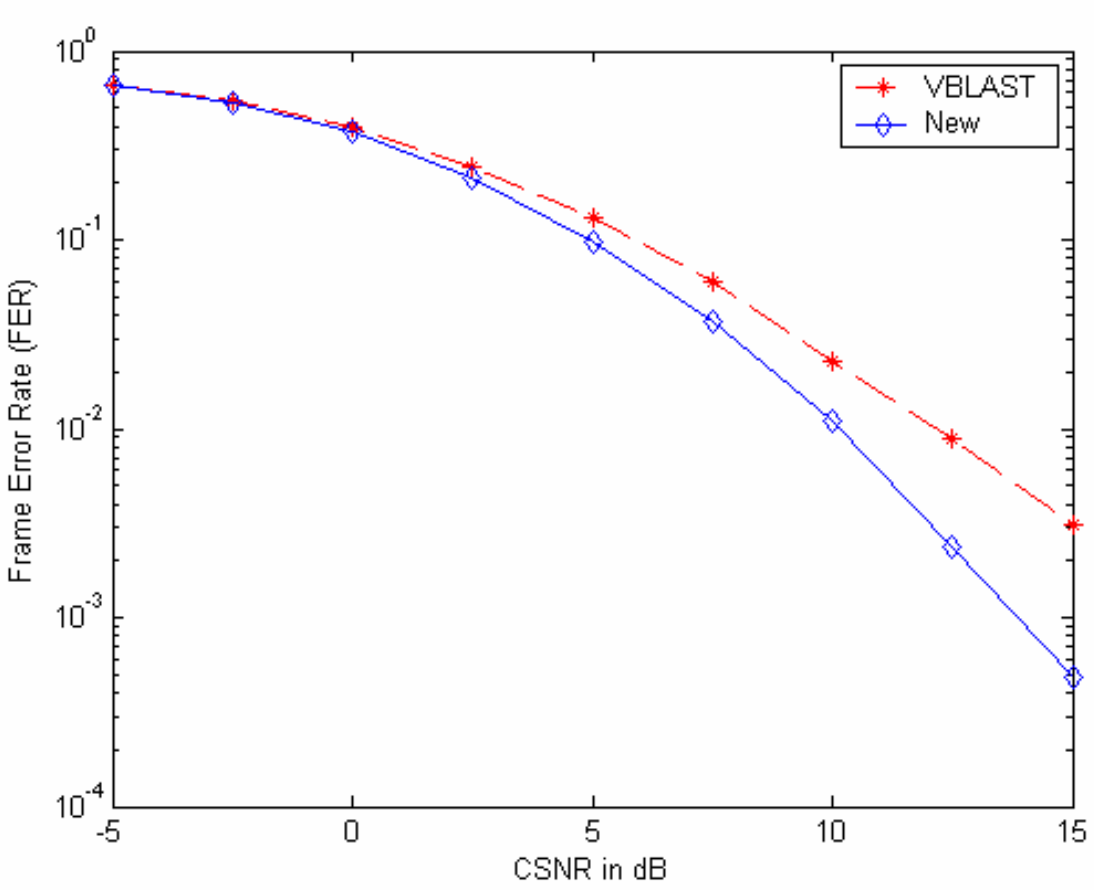

Figure 4.9 – BER for V-BLAST-BPSK, New-BPSK for 2 Tx, 2 Rx

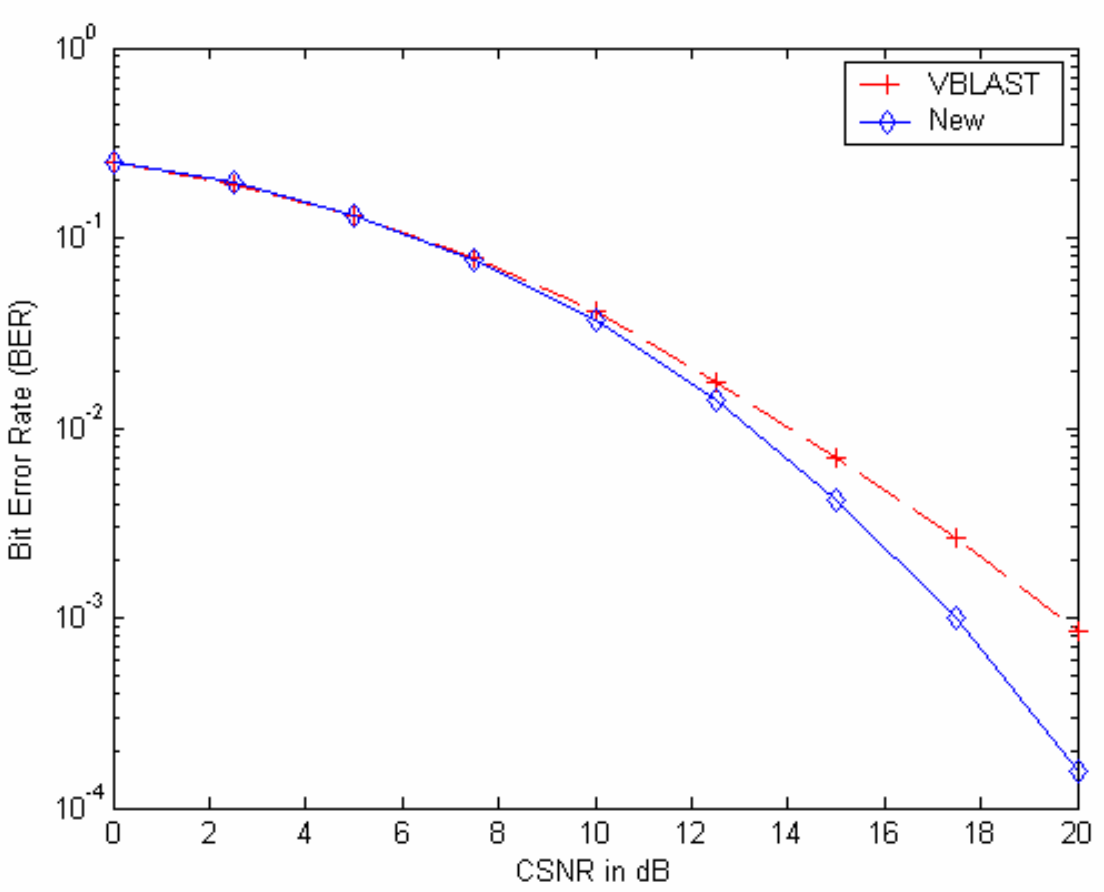

Figure 4.10 – FER for V-BLAST-BPSK, New-BPSK for 2 Tx, 4 Rx

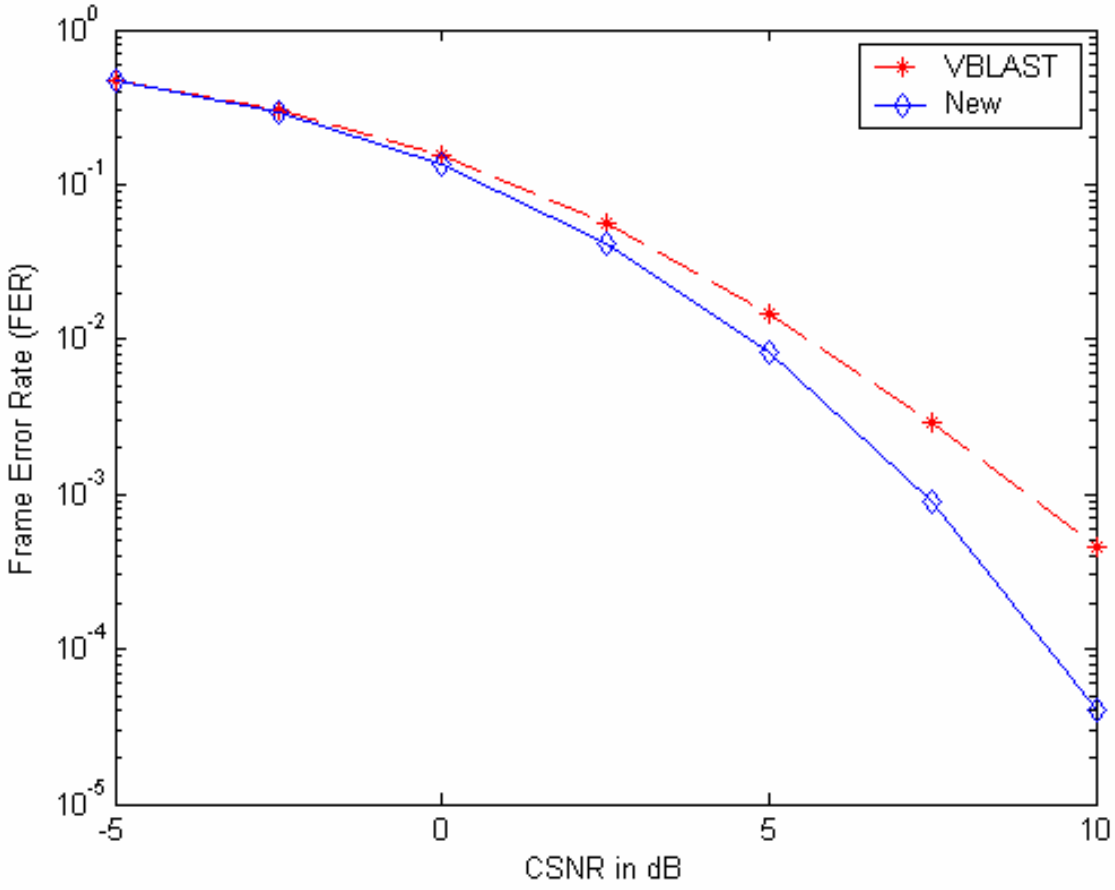

Figure 4.11 – BER for V-BLAST BPSK, New-BPSK for 2 Tx, 4 Rx

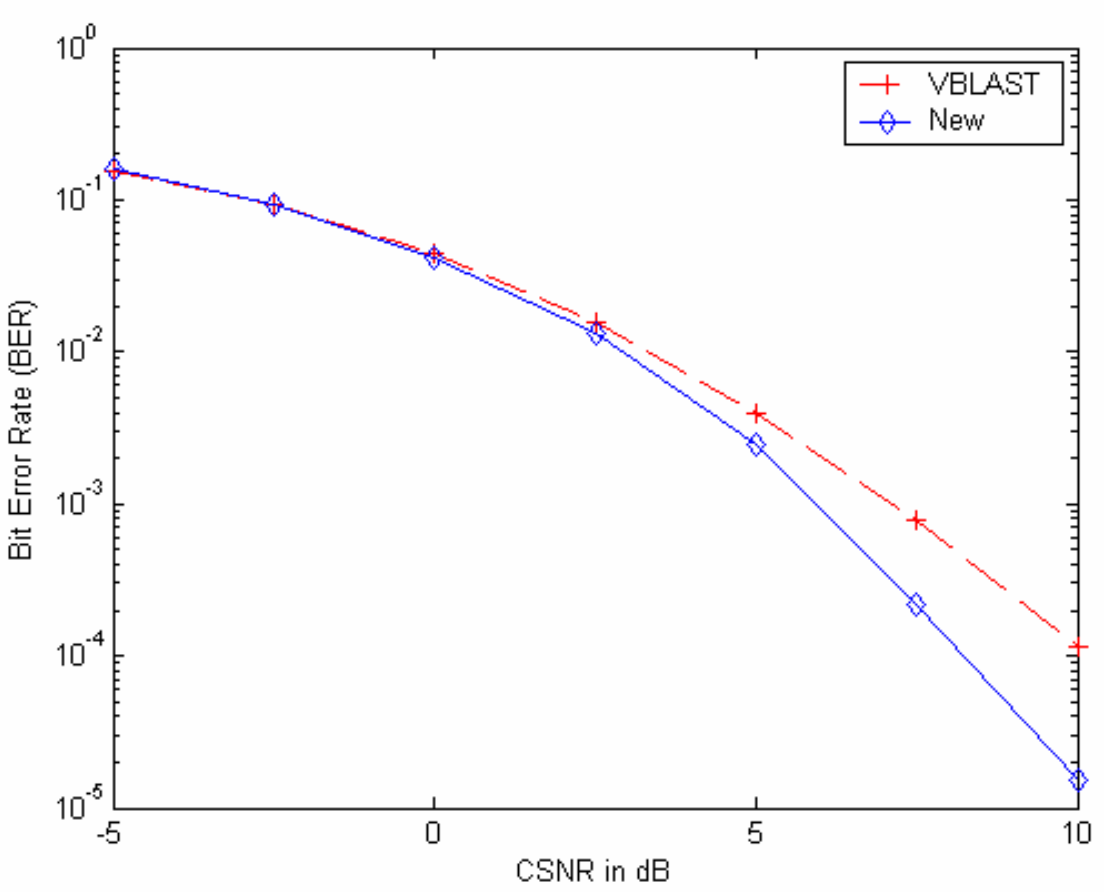

Simulation Results for LDC-Initialization

Figures 4.12-4.17 show FER and BER plots for the new LDC-initialized codes presented in (3.15), (3.16) and (3.17) with 1, 2 and 4 receive antennas, respectively, compared with the LDC code in (3.9).

Figure 4.12 – FER for LDC-BPSK, New-BPSK for 2 Tx, 1 Rx

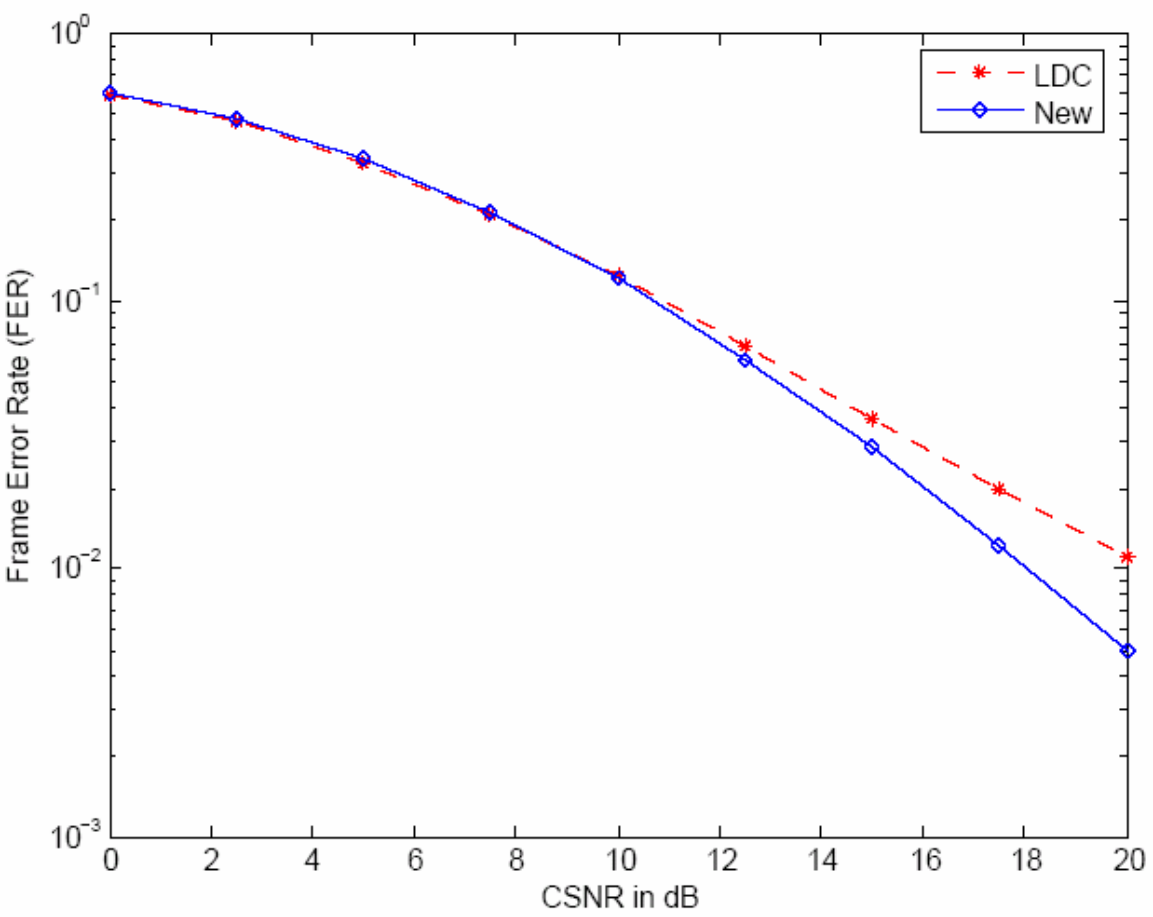

Figure 4.13 – BER for LDC-BPSK, New-BPSK for 2 Tx, 1 Rx

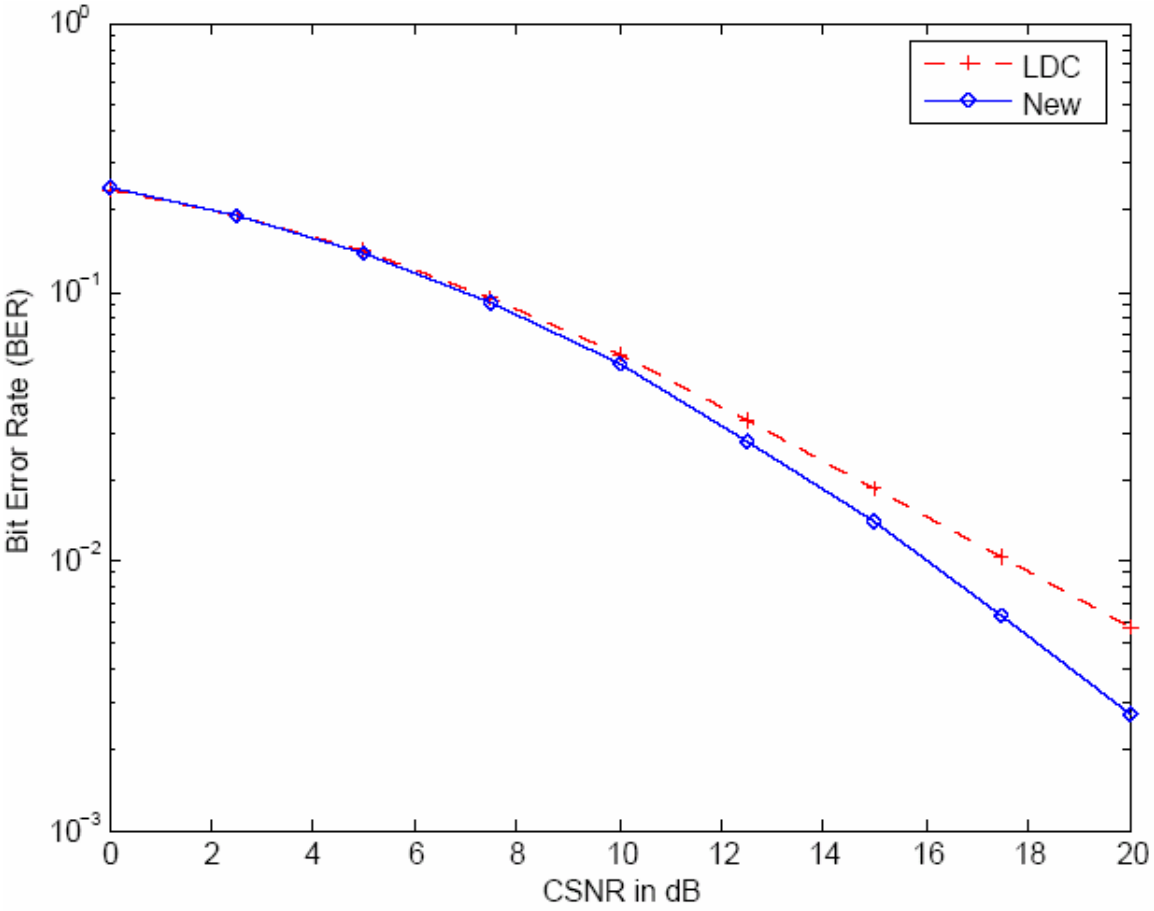

Figure 4.14 – FER for LDC-BPSK, New-BPSK for 2 Tx, 2 Rx

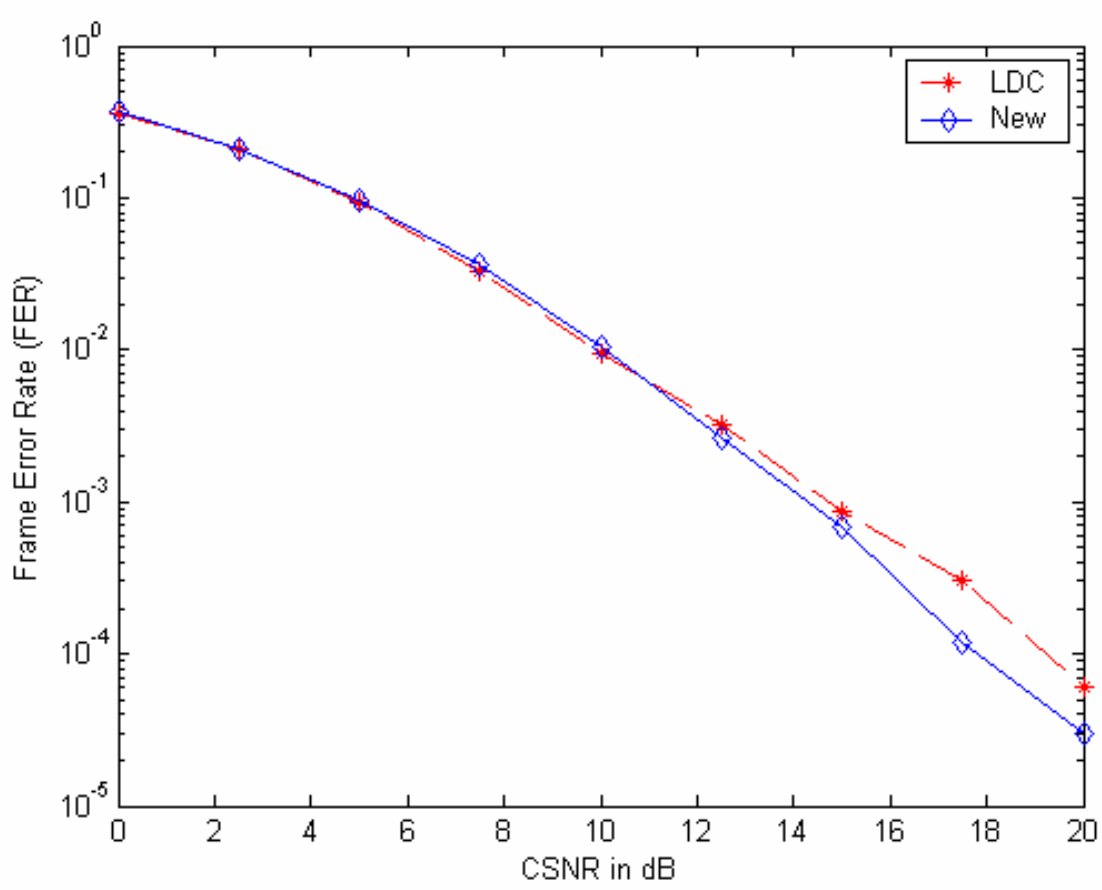

Figure 4.15 – BER for LDC-BPSK, New-BPSK for 2 Tx, 2 Rx

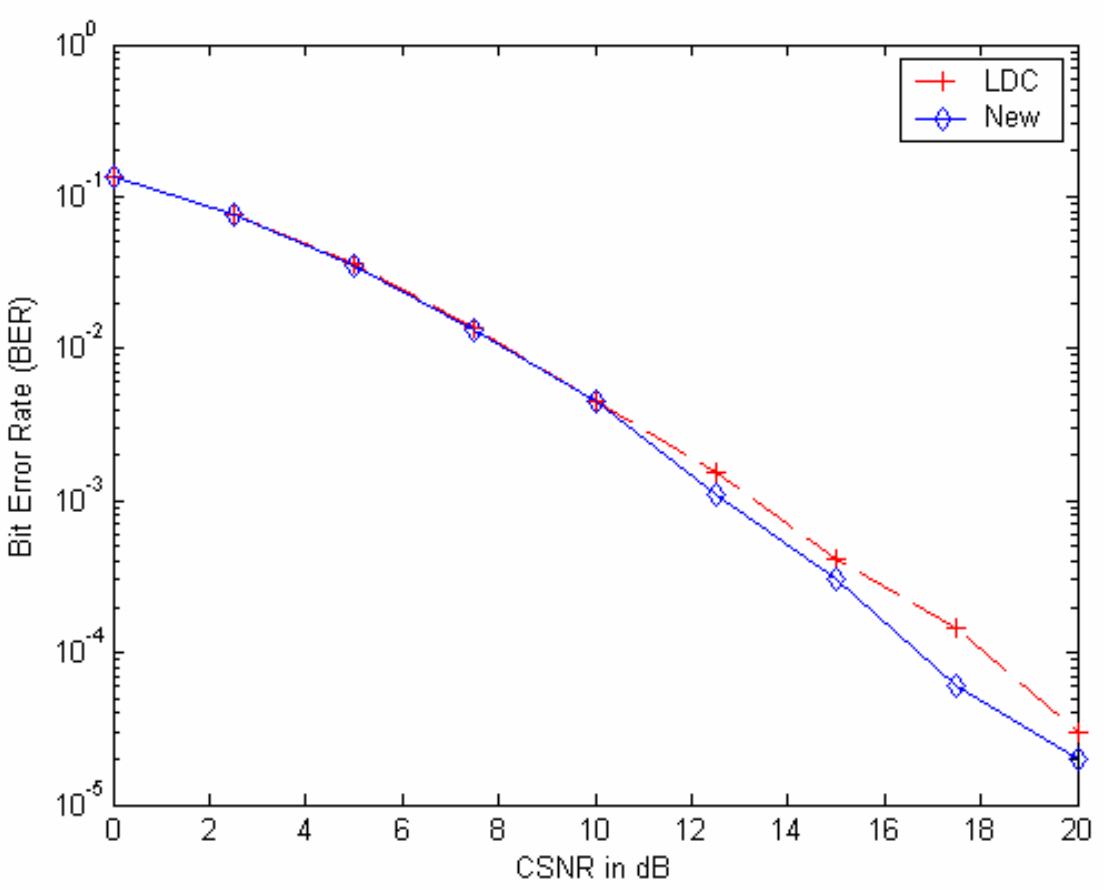

Figure 4.16 – FER for LDC-BPSK, New-BPSK for 2 Tx, 4 Rx

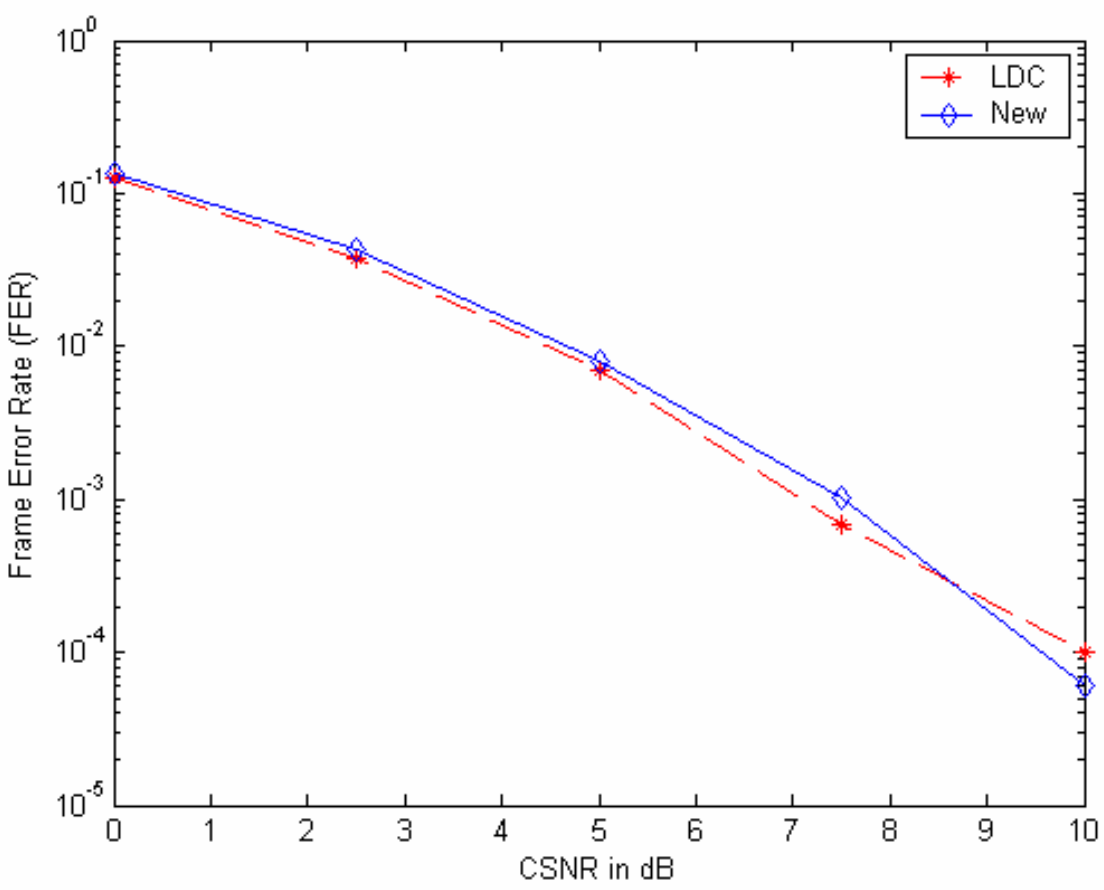

Figure 4.17 – BER for LDC-BPSK, New-BPSK for 2 Tx, 4 Rx

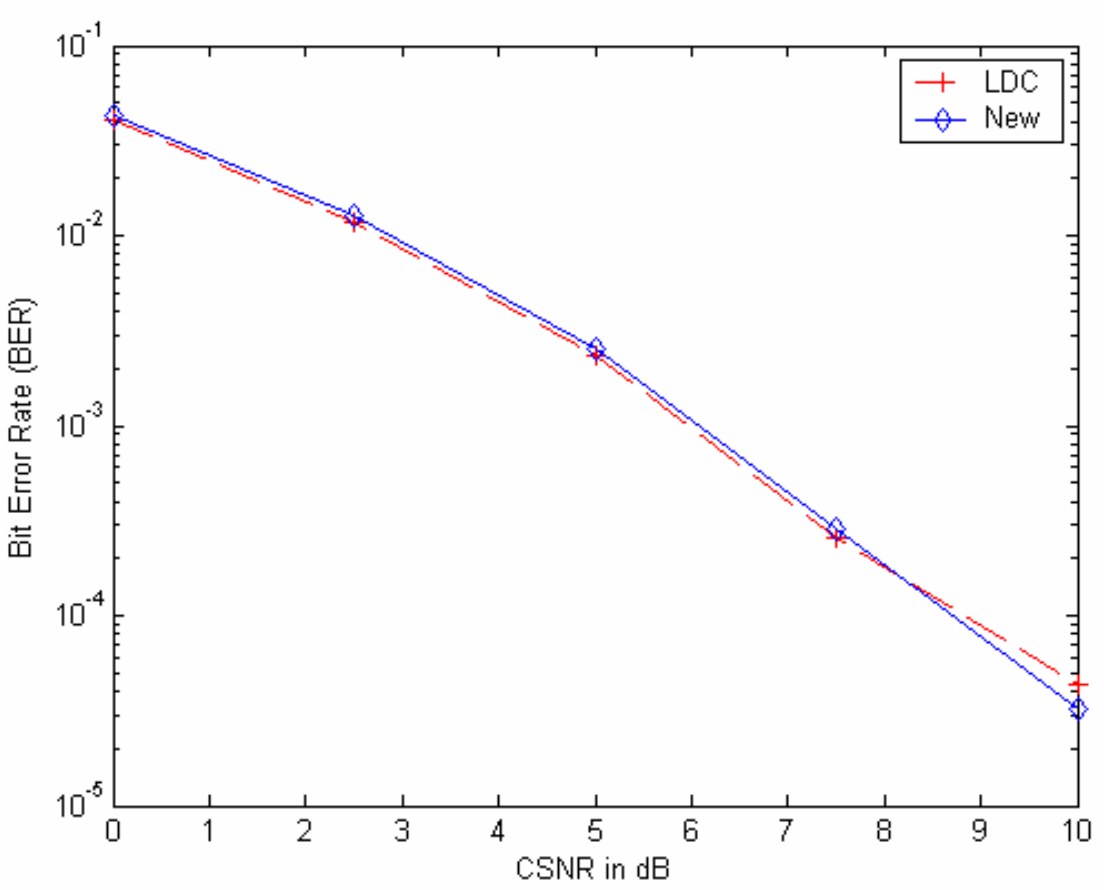

4.3 Discussion

Tables 4.1 and 4.2 provide summaries of the largest FER and BER gains, respectively, by the new codes observed in the simulation plots of Fig. 4.2-4.17.

Table 4.1 – Largest FER gains of new codes observed in simulation plots (in dB)

	$n_R = 1$	$n_R = 2$	$n_R = 4$
Alamouti	--	2.5	3
V-BLAST	5	3	2.5
LDC	2.5	Inconclusive	Inconclusive

Table 4.2 – Largest BER gains of new codes observed in simulation plots (in dB)

	$n_R = 1$	$n_R = 2$	$n_R = 4$
Alamouti	--	2.5	3
V-BLAST	2.5	2.5	2.5
LDC	2.5	Inconclusive	Inconclusive

These results show that the FER and BER performance of the new codes become increasingly better compared to Alamouti's code as the number of receive antennas goes up. For the V-BLAST simulations, we see that the new codes provide improved FER performance at a diminishing rate as the number of receive antennas goes up, going from a 5 dB gain at $n_R = 1$ to a

2.5 dB gain at $n_R = 4$, while maintaining a BER gain of 2.5 dB for all of the receive antenna cases tested. Finally, the LDC simulations show that the FER and BER advantage of the new codes is 2.5 dB for $n_R = 1$. No conclusion can be drawn for the $n_R = 2$ or 4 case due to the simulation FER and BER values being too small to produce reliable results for high CSNRs.

The FER gains observed in Table 4.1 are a direct result of our design methodology for the new codes, which aims to reduce the FER via a minimization of the FER union upper bound expression in (3.5). In contrast, Alamouti's code design objective was to produce OSTBCs with transmit and receive diversity which could produce diversity orders greater than the MRRC scheme. In designing V-BLAST, Wolniansky *et al.* sought to take advantage of the rich-scattering effects of multipath propagation to achieve high *spectral efficiency*, which is a measure of the number of bits per second that can be transmitted per Hz of bandwidth, while maintaining relatively simple decoding. Finally, the LDC code shown in (3.9) was designed by Hassibi *et al.* in order to maximize the mutual information between the input and output symbols. Though each of these three codes satisfies their respective design criteria, there was room for improvement when tested with our FER upper bound minimization criteria. In fairness, the new codes designed in this work were not tested with the conditions set out in [1], [27] and [11] and we have no reason to believe that those conditions would be satisfied, since our design did not take into consideration decoding complexity, high spectral efficiencies or mutual

information maximization between the transmitted and received symbols. An interesting extension of this work would be to test our newly designed codes under these criteria.

In our simulations, we also observe a significant discrepancy between the FER union upper bounds calculated in the design stage at 5 dB, shown in Tables 3.2-3.4, and the observed simulation FERs at a CSNR of 5 dB. Table 4.3 provides a summary of the findings.

Table 4.3 – Design FER upper bound compared with observed simulation FER

	Design FER upper bound at 5 dB	Simulation FER observed (approx.) at 5 dB
Alamouti		
$n_R = 2$	1.592608×10^{-1}	5.00×10^{-2}
$n_R = 4$	2.087142×10^{-2}	3.16×10^{-3}
$\mathbf{G}_{\text{NEW}}$, Alamouti-initialized		
$n_R = 2$	1.368865×10^{-1}	1.59×10^{-2}
$n_R = 4$	6.612724×10^{-3}	1.78×10^{-4}
V-BLAST		
$n_R = 1$	1.535247×10^{0}	2.51×10^{-1}
$n_R = 2$	5.188582×10^{-1}	1.12×10^{-1}
$n_R = 4$	9.444677×10^{-2}	1.12×10^{-2}
$\mathbf{G}_{\text{NEW}}$, V-BLAST-initialized		
$n_R = 1$	1.116808×10^{0}	2.40×10^{-1}
$n_R = 2$	2.676792×10^{-1}	1.00×10^{-1}

$n_R = 4$	2.001731×10^{-2}	6.31×10^{-3}
LDC		
$n_R = 1$	1.287384×10^{0}	1.78×10^{-1}
$n_R = 2$	3.610328×10^{-1}	1.00×10^{-1}
$n_R = 4$	5.391041×10^{-2}	5.01×10^{-3}
$\mathbf{G}_{\text{NEW}}$, LDC-initialized		
$n_R = 1$	1.110078×10^{0}	1.78×10^{-1}
$n_R = 2$	2.606916×10^{-1}	1.00×10^{-1}
$n_R = 4$	1.926679×10^{-2}	7.94×10^{-3}

This sizeable difference between the theoretical FER upper bound and the observed simulation FER upper bound suggests that there is room for lower upper bounds to be found in the design stage. We present this as an extension of this work.

Comments on other non-orthogonal codes

We have seen that our method of designing non-orthogonal STBCs by iteratively finding dispersion matrices A_i and B_i via random searches to minimize the FER union upper bound has produced encouraging results for the simple cases we have explored, that is, with BPSK modulation and only 2 transmit antennas. For more complex environments with larger constellation sizes and an increasing number of antennas, there exist strong-performing non-orthogonal codes, such as in Damen *et al.* [6], Lu *et al.* [17] and Maddah-Ali *et al.* [18]. The design of these codes takes into

account the determinant criterion and the rank criterion, established in [24], which aim to minimize the worst-case PEP between two codewords by establishing guidelines to optimize coding gain and diversity gain, respectively. In contrast, our design considers the entire error probability term, not just between two codewords, and uses an exact PEP expression (2.32) rather than a worst-case bound. Our approach provides increasingly accurate error probability performance as the CSNR rises.

Comparisons with [6], [17] and [18] were not made in this work but we propose it as an interesting research opportunity. We note that the design technique presented in this work cannot increase the FER union upper bound of the initial code but can only improve it or, in the worst-case, keep it the same. However, we have seen in the case of the LDC comparison that a lower FER union upper bound in the design stage does not guarantee stronger FER performance in simulation, due to the looseness of the bound.

Comments on complexity

In Section 2.6 we commented on the comparative decoding complexity of orthogonal codes versus non-orthogonal codes. In our designs, Alamouti's code uses a QPSK modulation to transmit 2 symbols per block, i.e. $M = 4$ and $k = 2$, which could be decoded efficiently in $2 \times 4 = 8$ detections. For the new codes, we used BPSK modulation ($M = 2$) and transmitted 4 symbols per block ($k = 4$), requiring $2^4 = 16$ ML detections to decode. Hence, even in

our simple setup, the decoding complexity is twice as high for our non-orthogonal linear codes compared with the orthogonal block code designs.

Chapter 5

Conclusions & Future Work

5.1 Summary

In Chapter 2, we presented background material on communication channel models and information theory before establishing a multiple-antenna system model. We also presented orthogonal and non-orthogonal space-time block code designs. For OSTBCs, we started with a description of Alamouti's simple two-branch diversity scheme and how it inspired Tarokh *et al.* to generalize this method for any number of transmit antennas. These orthogonal codes offer a variety of benefits, including linear processing at the decoder and full diversity gains. However, complex orthogonal designs that achieve high rate (>1/2) are difficult to construct for arbitrary numbers of transmit antennas. NOSTBCs loosen the orthogonality conditions in codeword design in

exchange for codes that can achieve full rate for any number of antennas. In the case of LDCs, we saw that the design parameters, the dispersion matrices A_i, B_i and Q, were chosen in order to maximize the mutual information between the input and output symbols. The tradeoff of high-rate achievability in NOSTBCs comes at the price of exponential decoding complexity, versus linear complexity for OSTBCs. In this chapter, we also defined the concept of pairwise error probability as the probability of erroneously decoding a codeword $\hat{\mathbf{S}}$ when $\mathbf{S}$ was transmitted. We presented Behnamfar's derivation of a general formula for the PEP which relies on the residues of the MGF of the squared-distance expression between two codewords.

In Chapter 3, we proposed a new NOSTBC based on minimizing error rate performance using the LDC structure of [11], unlike the LDCs by Hassibi *et al.* who chose design parameters based on maximizing mutual information. We defined the FER and BER and expressed both in terms of a probability of a union of events and used the union bound in the FER expression to form an upper bound. The union bound relies on the pairwise error probability equation derived in the previous chapter.

The new $\mathbf{G}_{\text{NEW}}$ codes were designed for a CSNR of 5 dB and for $T = n_T = 2$ through an iterative random search process of finding dispersion matrices that produced progressively lower FER union upper bounds.

Three such designs were formed by initializing with Alamouti's $\mathbf{G}_2$ code, V-BLAST and an LDC code from [11]. For the Alamouti-initialization, the relaxed orthogonality conditions in the new codes produced lower FER upper bounds for the $n_R = 2$ and 4 cases. For the case of 1 receive antenna, the $\mathbf{G}_{\text{NEW}}$ code could not provide a lower FER bound than the $\mathbf{G}_2$ code. This result is due to the fact that Alamouti's code maximizes the mutual information under this system setup for orthogonal codes with $n_T = 2$ and $n_R = 1$. For the V-BLAST and LDC-initializations, lower FER upper bounds were found for $n_R = 1, 2$ and 4. Overall, the design results indicated that as the number of receive antennas is increased, so does the potential improvement in the FER union upper bound in the new codes.

The resulting $\mathbf{G}_{\text{NEW}}$ codes from Chapter 3 were tested in simulations whose results were presented in Chapter 4. The simulation took in the dispersion matrices from the code designs and produced an indexed codebook. For a given CSNR, a random codeword index was transmitted and subjected to channel fading and noise and detected by an ML decoder. This process was repeated 5×10^4 times for each CSNR in a range and the FER and BER were calculated and plotted for each $\mathbf{G}_{\text{NEW}}$ versus the code used to initialize it.

The resulting plots showed a significant improvement in the FER and BER performance of the $\mathbf{G}_{\text{NEW}}$ codes over the $\mathbf{G}_2$ code, with gains of 2.5 dB and 3 dB for the cases of 2 and 4 receive antennas, respectively. This trend indicates that as the number of receive antennas is increased, the error rate advantage of $\mathbf{G}_{\text{NEW}}$ over $\mathbf{G}_2$ increases. The simulation plots for the V-BLAST-initialization showed the opposite trend. Starting with a performance gain for $\mathbf{G}_{\text{NEW}}$ of 5 dB over V-BLAST when $n_R = 1$, the advantage diminished to 3 dB when $n_R = 2$ and down to 2.5 dB when $n_R = 4$. This leads us to conclude that as the number of receive antennas goes up, the error rate performance of $\mathbf{G}_{\text{NEW}}$ gets weaker compared to V-BLAST. Finally in the LDC-initialization, $\mathbf{G}_{\text{NEW}}$ provided a 2.5 dB advantage over the LDC for the 1 receive antenna case. For the case of 2 and 4 receive antennas, no conclusive claim can be made since the FER and BER values became too low to be reliable at higher CSNRs.

In all three design scenarios above, it was also observed that the simulation FER at the design target CSNR of 5 dB was considerably smaller than the calculated FER upper bounds in the design stage, leading us to conclude that tighter upper bounds on the FER can and should be found.

5.2 Future Work

This work introduced an approach to producing non-orthogonal linear-STBCs via FER union upper bound minimization. There are many different research opportunities available to extend the work presented here. Such opportunities include:

- Designing non-orthogonal linear-STBCs via the method described in this work that utilize larger complex constellations, such as 8-PSK and 16-QAM.
- Use a more advanced search technique for dispersion matrices $\{A_q, B_q\}$, such as *simulated annealing* which allows non-improving replacements with diminishing probability over time to increase the chance of not getting 'stuck' in a local minimum.
- Use a tighter upper bound than the union bound for the probability of a union of events, such as Hunter's bound in [13].
- In the code design, one could initialize with other non-orthogonal codes that were designed for error rate minimization, such as Damen's code in [6], Lu's code in [17] or the Maddah-Ali code in [18].

Bibliography

[1] S.M. Alamouti, "A simple transmitter diversity scheme for wireless communications", *IEEE J. Select Areas Communications*, vol. 16, pp. 1451-1458, Oct. 1998.

[2] F. Behnamfar, "Single and Multiple Antenna Communication Systems: Performance Analysis and Joint Source-Channel Coding", Ph.D. Dissertation, Dept. of Electrical & Computer Engineering, Queen's University, Kingston, Canada, Sept. 2004.

[3] F. Behnamfar, F. Alajaji and T. Linder, "Tight Error Bounds for Space-Time Orthogonal Block Codes under Slow Rayleigh Flat Fading", *IEEE International Symposium on Information Theory*, June-July 2003, Yokohama, Japan.

[4] T. Cover and J. Thomas, *Elements of Information Theory*, Wiley, 1991.

[5] L. A. Dalton and C. N. Georghiades, "A Full-Rate, Full-Diversity Four Antenna Quasi-Orthogonal Space-Time Block Code", *IEEE Trans. Wireless Comm.*, vol. 4, no. 2, March 2005.

[6] M. O. Damen, A. Tewfik and J.C. Belfiore, "A construction of a space-time code based on number theory", *IEEE Trans. Inform. Theory*, vol. 48, pp. 753-760, Mar. 2002.

[7] G.J. Foschini, "Layered space-time architecture for wireless communication in a fading environment when using multi-element antennas", *Bell Labs Tech. J.*, vol. 1, no. 2, pp 41-59, Autumn 1996.

[8] G.J. Foschini, Jr. and M.J. Gans, "On limits of wireless communication in a fading environment when using multiple antennas", *Wireless Personal Commun.*, vol. 6, pp. 311-335, 1998.

[9] A. Grant, "Rayleigh Fading Multi-Antenna Channels", *EURASIP Special Issue on Space-Time Coding*, May 29, 2001.

[10] L. Hanzo, T. H. Liew and B. L. Yeap, *Turbo Coding, Turbo Equalisation and Space-Time Coding for Transmission over Fading Channels*, John Wiley & Sons Ltd., 2002.

[11] B. Hassibi and B.M. Hochwald, "High-rate codes that are linear in space and time", *IEEE Trans. Inform. Theory*, vol. 48, no. 7, July 2002.

[12] R. W. Heath, Jr. and A. J. Paulraj, "Linear Dispersion Codes for MIMO Systems Based on Frame Theory", *IEEE Trans. On Signal Process.*, vol. 50, no. 10, October 2002.

[13] D. Hunter, "An upper bound for the probability of a union", *J. Appl. Probab.*, vol. 13, pp. 597-603, 1976.

[14] H. Jafarkhani, "A Quasi-Orthogonal Space-Time Block Code", *IEEE Trans. On Commun.*, vol. 49, No. 1, January 2001.

[15] H. Kan and H. Shen, "A Counterexample for the Open Problem on the Minimal Delays of Orthogonal Designs With Maximal Rates", *IEEE Trans. Inform. Theory,* vol. 51, no. 1, January 2005.

[16] E.G. Larsson and P. Stoica, *Space-Time Block Coding for Wireless Communications*, Cambridge University Press, 2003.

[17] H. Lu, Y. Wang, P. V. Kumar and K. M. Chugg, "Remarks on Space-Time Codes Including a New Lower Bound and an Improved Code", *IEEE Trans. Inform. Theory*, vol. 49, No. 10, October 2003.

[18] M. A. Maddah-Ali and A. K. Khandani, "A New Space-Time Code Based on Permutation Matrices", *CWIT 2003*, Waterloo, Canada, May 2003.

[19] J.G. Proakis, *Digital Communications*, McGraw-Hill, 2001.

[20] T.S. Rappaport, *Wireless Communications - Principles and Practice*. Prentice Hall PTR, 1996.

[21] C. Schlegel and Z. Bagley, "MIMO Channels & Space-Time Coding", *WOC 2002*, Banff, Canada, July 2002.

[22] W. Su and X-G Xia, "Two Generalized Complex Orthogonal Space-Time Block Codes of Rates 7/11 and 3/5 for 5 and 6 Transmit Antennas", *IEEE Trans. Inform. Theory*, vol. 49, no. 1, January 2003.

[23] G. Taricco and E. Biglieri, "Exact pairwise error probability of space-time codes", *IEEE Trans. Inform. Theory*, vol. 48, pp. 510-513, Feb. 2002.

[24] V. Tarokh, N. Seshadri and A.R. Calderbank, "Space-time codes for high data rate wireless communication: Performance criterion and code construction", *IEEE Trans. Inform. Theory*, vol. 44, no. 2, pp. 744-765, Mar. 1998.

[25] V. Tarokh, H. Jafarkhani and A.R. Calderbank, "Space-time block codes from orthogonal designs", *IEEE Trans. Inform. Theory*, vol. 45,

no. 5, July 1999.

[26] E. Telatar, “Capacity of multiple-antenna Gaussian channels”, *Europ. Trans. Telecommun.*, vol. 10, pp. 585-595, Nov. 1999.

[27] P. W. Wolniansky, G. J. Foschini, G. D. Golden and R. A. Valenzuela, “V-BLAST: An Architecture for Realizing Very High Data Rates Over the Rich-Scattering Wireless Channel”, *Proc. ISSSE-98*, Italy, Sept. 1998.

[28] Ziemer, R. E. and Peterson, R. L., *Introduction to Digital Communication*, Macmillan Publishing Company, 1992.